

日中笹川医学奨学金制度(学位取得コース)評価書

課程博士：指導教官用



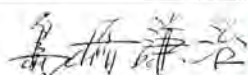
第 42 期

研究者番号： G4206

作成日： 2022 年 3 月 日

氏名	Meng Huachuan	孟 華川	性別	M	生年月日	1985. 02. 04
所属機関(役職)	中日友好医院院外国際交流合作弁公室(通訳(日本プロジェクト担当))					
研究先(指導教官)	国際医療福祉大学大学院医療福祉経営専攻 医療経営管理分野(島崎 謙治教授) 国際医療福祉大学大学院医学研究科 医学専攻(桐生 茂教授)					
研究テーマ	遠隔医療の導入効果及び推進方策(副題)日本の遠隔画像診断の中国への展開を中心に Effects of introducing telemedicine and promotion strategies: Focusing on developing teleradiology for remote diagnosis for patients in China from Japan					
専攻種別	<input type="checkbox"/> 論文博士			<input checked="" type="checkbox"/> 課程博士		

研究者評価(指導教官記入欄)

成績状況	<input checked="" type="checkbox"/> 優 <input type="checkbox"/> 良 <input type="checkbox"/> 可 <input type="checkbox"/> 不可 学業成績係数= 2.67	取得単位数 34.0/12.0 必要単位数は取得済み。
学生本人が行った研究の概要	<p>① 文献調査による日本の遠隔画像診断に関する事業の市場特性の分析。</p> <p>② アンケート調査及びインタビュー調査による大学病院や民間企業の遠隔画像診断の国際展開とりわけ中国への展開の海外の意向及び阻害要因の分析。</p> <p>③ 日本及び中国の医事法制及び情報セキュリティに関する法規制の分析と遠隔画像診断の中国への展開における法的リスクの考察。</p> <p>④ 国をまたがる遠隔画像診断の展開に関する日本及び中国に対する政策提言の考察・検討。</p>	
総合評価	<p>【良かった点】 COVID-19の蔓延によりアンケート調査及びインタビュー調査等の実施が大きく制約されるなかで、本人の様々な人的ネットワークを活用して調査の実施に漕ぎ着けた。また、遠隔医療や情報セキュリティ関係に関する日本及び中国の法令の改廃が頻繁に行われているなかで、改正法令の詳細な分析や事業スキームの法的リスク等の考察を行い、副論文を仕上げ学会誌に投稿した。</p> <p>【改善すべき点】 本人の大学時代の専攻など経歴上やむを得ない面もあるが、事象を分析・整理し、その結果を論理的に組み立て、首尾一貫した論文にまとめ上げる能力を一層磨く必要があると思われる。また、研究に限らず、質問に対し短時間で要点を整理し要領よく回答する訓練を積むことが望まれる。これは口頭試問対策としても重要である。</p> <p>【今後の展望】 COVID-19により来日が遅れたことや調査の実施スキームの変更を余儀なくされたこともあって、博士課程に入学したときに想定していたスケジュールに比べ、やや遅れ気味である。しかし、今後、研究のピッチを更に上げ、所期の目的を達成できるよう督励したい。</p>	
学位取得見込	投稿中の副論文の内容は本論文においても重要な部分を占める。今後、アンケート調査及びインタビュー調査の結果をまとめるとともに、遠隔画像診断の市場分析の補充等を行うことにより、学位論文の申請に漕ぎ着けたい。	
評価者(指導教官名)	国際医療福祉大学教授	 

日中笹川医学奨学金制度(学位取得コース)報告書 研究者用



第42期

研究者番号: G4206

作成日: 2022年3月 6 日

氏名	Meng Huachuan	孟 華川	性別	M	生年月日	1985. 02. 04
所属機関(役職)	中日友好医院院弁国際交流合作弁公室(通訳(日本プロジェクト担当))					
研究先(指導教官)	国際医療福祉大学大学院医療福祉経営専攻 医療経営管理分野(島崎 謙治教授) 国際医療福祉大学大学院医学研究科 医学専攻(桐生 茂教授)					
研究テーマ	遠隔医療の導入効果及び推進方策(副題)日本の遠隔画像診断の中国への展開を中心に Effect of introducing telemedicine and promotion strategies: Focusing on developing teleradiology for remote diagnosis for patients in China from Japan					
専攻種別	論文博士	<input type="checkbox"/>	課程博士	<input checked="" type="checkbox"/>		

1. 研究概要(1)

① 研究の背景

近年、ICT(情報通信技術)の急速な進展を背景に、遠隔医療の技術的障壁が小さくなるとともに、医療資源の地域格差が拡大するなかで、遠隔診療に対する期待・関心が高まっている。遠隔医療が日本及び中国で注目されている理由としては、①人口当たり医師数は増加しているが、医師や医療機関の地域間格差はむしろ増大している。遠隔医療は医療資源の偏在の克服に寄与されることが期待されている。②日中とも高齢化が進んでいる。高齢者は糖尿病、高血圧など慢性疾患の罹患率が高い。遠隔医療はこうした患者の継続的診療に有用である。(参考)高齢化率 日本:28.1%(2018)→35.3%(2040年推計) 中国:17.9%(2018)→約30%(2042推定) ③近年のICT技術の飛躍的な進展により、遠隔診療の技術的基盤が整備・充実されてきた。このように遠隔診療に関する規制緩和等は急速に進展しているが、患者の医療へのアクセスの改善、通院や訪問診療の移動コストの削減、診療回数の増加による医療の質の向上等の点で、遠隔診療は大きなポテンシャルを有していると考えられる。遠隔医療の最大のメリットは、医師と患者が異なる場所においても診療が可能にあることにある。これは遠隔医療が国境を越えて発展するポテンシャルを有することを意味する。実際、経済産業省の後押しもあり、遠隔医療の国際展開を図っている医療機関や事業者もある。しかし、その評価や課題などの分析は十分行われていない。とくに、国をまたがる遠隔医療は国内で完結する場合は異なる難しさがある。それは医療の慣習や言語が異なることだけではない。より本質的な難しさは、遠隔医療に関する各国の法規制が異なり、かつ、その適用が輻輳化することにある。

本研究では遠隔画像診断の中国への展開を中心に分析・考察を行う。遠隔画像診断を取り上げる理由は、①現状でも遠隔画像診断は遠隔医療市場の大きなシェア(推計ベースで約8割)を占めていること、②日本の画像診断の技術水準は高く国際的競争力を有すること、③言語や慣習の相違に起因するトラブルが比較的生じにくく海外展開のポテンシャルが大きいことによる。また、中国を対象とする理由は、①中国は人口規模が大きい上に都市と農村部の医療格差が大きく遠隔画像診断の需要が大きいこと、②日本の画像診断技術は中国でも高く評価されていること、③中国では遠隔医療を推進する一方、個人情報データの国内保存の義務づけ等の法規制が急速に進められており、日本が遠隔画像診断の展開を進める上で法的リスクの分析・考察が不可欠であることによる。

② 先行研究

日本の先行研究としては、地方医療支援と地域格差の解消を手段とする遠隔医療の効果を中心に論じた吉田・亀畑(1998)、遠隔医療の法的問題を考察した河原(2003)、樋口(2007)、遠隔医療の海外展開に伴う民事責任を論じた山下(2008)の研究などがある。また、中国の先行研究としては、遠隔医療の規制を論じた司・趙(2017)、遠隔医療の侵権責任(日本の不法行為責任に相当)の分担を論じた熊(2020)などがある。これらの先行研究の多くは遠隔医療に関する法的規制と規制緩和などについて論じたものであり、遠隔画像診断に特化し、かつ、日本および中国の最新の法規制等の情報に基づき分析・検討した研究は乏しい。

③ 本研究の位置づけ

遠隔医療とりわけ遠隔画像診断は国内のみならず国際的に展開するポテンシャルがあり、その導入効果・課題および推進方策を明らかにすることは、学術的・医療政策的に大きな意義がある。

1) 目的(Goal)

本研究の目的は、遠隔医療とりわけ遠隔画像診断の導入効果および普及を図るための課題の分析・考察を行うとともに、日本が遠隔画像診断を中国で展開する場合の法的リスクの分析とその解消方策を検討するなど、遠隔画像診断の推進方策について論考・提言することである。

2) 戦略(Approach)

ステップ①: 先行研究のレビュー、日本および中国の遠隔医療の現状の分析、日本の遠隔画像診断の市場特性や中国に展開する場合の課題等に関する文献調査を行う。

1. 研究概要(2)

ステップ②: アンケート調査とインタビュー調査を実施し、遠隔医療の導入効果、課題(法的リスク)、普及の阻害要因(政策面・技術面・人的資源など)を明らかにする。

ステップ③: 最新文献とデータ解析を通して、日本が遠隔画像診断を中国で展開する場合の法的リスクの分析とその解消方を検討するなど、遠隔画像診断の推進方策について論考・提言する。

3) 材料と方法(Materials and methods)

① 中国及び日本で公刊された書籍、論文や日中両国の法令及び指針など公開済みの情報と先行研究を踏まえ、調査報告をまとめる。

② アンケート調査(日本60施設)とインタビュー調査(日本8施設、中国8施設)を実施し、結果の回収・解析を行った。

4) 実験結果(Results)

1. 主論文について

法整備(医師法)や診療報酬、補助金及び税政上の優遇策が不十分などの制度面の制約だけでなく、個人情報やデータ管理のリスク、インシヤルコスト及びランニングコストが高い等が、日本及び中国の遠隔医療普及の大きな阻害要因となっている。医療機関及び事業者にとって、遠隔画像診断を導入することによって、専門医による迅速な読影ができるため、地域医療の質の向上に寄与できること、送信側の医療機関の医師にとって教育効果があること、地域の中核病院と一般病院との役割分担が行われ、地域医療の効率化が図られること等の効果が期待できる。今後、日中間の遠隔画像診断を発展させるためには、法整備や診療報酬の充実及び診療に関するデータの国外移転について特例措置を講じること等が望まれる。

2. 副論文について

D-Pの場合、Pの主治医が介在せずにDがPの医学的情報を十分把握することは難しく、日本及び中国の医師法に違反すると考えられる。D₂-D₁-Pの場合、日本の医師法上は、D₂の行為はD₁に対する単なる助言だと解釈されており同法に違反しない。このスキームは中国の医師法上も合法であるが、Pの診断に関しD₂はD₁と共同責任を負うとともに、D₂の読影ミスがあればPから不法行為に関する訴訟を提起されるリスクがある。また、D₁はPの病歴や画像等の国内保存義務の回避措置(個人情報及び重要データの国外移転の安全評価手続)をとる必要がある。

5) 考察(Discussion)

本稿では、日本の遠隔画像診断の中国への展開を中心に、遠隔医療の導入効果及び推進方策等を分析・検討した。考察で以下のようなことが明らかになった。① 日本で、遠隔画像診断を実施している国公立大学病院は少ない。その理由は、インシヤルコストや日々の診療業務との兼合い等の課題があるほか、遠隔画像診断を行っている民間企業等もあり競争が激しい中でリスク判断が難しいこと等が考えられる。②、NPO法人を設立し遠隔画像診断を行うケースや私立大学病院が法人の経営戦略として遠隔画像診断を実施するケースがみられる。③ 設立形態・立地条件、経営トップのイニシアティブ等によって、遠隔画像診断の実績及び国際展開の経営戦略が異なる。④ 遠隔画像診断の国内市場ニーズは飽和状態に近い一方、国際的には有望な市場であり、一部の私立病院や大学発ベンチャー法人等が国際展開を実施あるいは検討している。ただし、相手国の医事法制や個人情報保護等の法的リスクの懸念がある。

6) 参考文献(References)

1) 矢野経済研究所. 2021年版遠隔医療市場の将来展望. 2021:11-12

2) 厚生労働省. 2019. 「オンライン診療の適切な実施に関する指針」に関するQ&A.

<https://www.mhlw.go.jp/content/000534139.pdf>. 2021.11.10

3) 于佳佳. 远程医疗对我国现行法律适用之挑战. 中国社会科学院研究生院学报2018;(3):125-134. (論文名の日本語訳: 遠隔医療の我が国の現行法適用に対するチャレンジ)

4) 瓜生・糸賀法律事務所. 個人情報越境移転の法務. 東京. 中央経済社, 2020

5) 日本医学放射線学会. 2019. 遠隔画像診断に関するガイドライン

2018. http://www.radiology.jp/content/files/20190218_01.pdf. 2021.12.15

6) 経済産業省. 2020. 中国の健康診断・人間ドック受診患者に対する、日本人専門医師による遠隔画像診断拠点化プロジェクト事業報告書. 24. https://www.meti.go.jp/policy/mono_info_service/healthcare/iryuu/outbound/area/china.html. 2021.11.23

7) 樋口範雄. 医療と法を考える: 救急車と正義. 東京. 有斐閣, 2007:86-106

8) 山下登. 医師の民事責任をめぐる新たな一局面: 遠隔診療をめぐるドイツの法状況を手がかりとして. 岡山大学法学会雑誌2008;57(4):722-744

9) 笹山桂一. 医療における新しい診療手法と法的問題: 遠隔診療とAIを中心に. 先端技術・情報の企業化と法. 東京. 文眞堂, 2020:198-213

10) 日本医学放射線学会. 2019. 遠隔画像診断に関するガイドライン

2018. http://www.radiology.jp/content/files/20190218_01.pdf. 2021.12.15

11) 厚生労働省. 2019. 「オンライン診療の適切な実施に関する指針」に関するQ&A.

<https://www.mhlw.go.jp/content/000534139.pdf>. 2021.11.10

2. 執筆論文 Publication of thesis ※記載した論文を添付してください。Attach all of the papers listed below.

論文名 1 Title						
掲載誌名 Published journal						
	年	月	巻(号)	頁 ~	頁	言語 Language
第1著者名 First author			第2著者名 Second author			第3著者名 Third author
その他著者名 Other authors						
論文名 2 Title						
掲載誌名 Published journal						
	年	月	巻(号)	頁 ~	頁	言語 Language
第1著者名 First author			第2著者名 Second author			第3著者名 Third author
その他著者名 Other authors						
論文名 3 Title						
掲載誌名 Published journal						
	年	月	巻(号)	頁 ~	頁	言語 Language
第1著者名 First author			第2著者名 Second author			第3著者名 Third author
その他著者名 Other authors						
論文名 4 Title						
掲載誌名 Published journal						
	年	月	巻(号)	頁 ~	頁	言語 Language
第1著者名 First author			第2著者名 Second author			第3著者名 Third author
その他著者名 Other authors						
論文名 5 Title						
掲載誌名 Published journal						
	年	月	巻(号)	頁 ~	頁	言語 Language
第1著者名 First author			第2著者名 Second author			第3著者名 Third author
その他著者名 Other authors						

3. 学会発表 Conference presentation ※筆頭演者として総会・国際学会を含む主な学会で発表したものを記載してください

※Describe your presentation as the principal presenter in major academic meetings including general meetings or international meetings

学会名 Conference					
演題 Topic					
開催日 date	年	月	日	開催地 venue	
形式 method	<input type="checkbox"/> 口頭発表 Oral	<input type="checkbox"/> ポスター発表 Poster	言語 Language	<input type="checkbox"/> 日本語	<input type="checkbox"/> 英語 <input type="checkbox"/> 中国語
共同演者名 Co-presenter					
学会名 Conference					
演題 Topic					
開催日 date	年	月	日	開催地 venue	
形式 method	<input type="checkbox"/> 口頭発表 Oral	<input type="checkbox"/> ポスター発表 Poster	言語 Language	<input type="checkbox"/> 日本語	<input type="checkbox"/> 英語 <input type="checkbox"/> 中国語
共同演者名 Co-presenter					
学会名 Conference					
演題 Topic					
開催日 date	年	月	日	開催地 venue	
形式 method	<input type="checkbox"/> 口頭発表 Oral	<input type="checkbox"/> ポスター発表 Poster	言語 Language	<input type="checkbox"/> 日本語	<input type="checkbox"/> 英語 <input type="checkbox"/> 中国語
共同演者名 Co-presenter					
学会名 Conference					
演題 Topic					
開催日 date	年	月	日	開催地 venue	
形式 method	<input type="checkbox"/> 口頭発表 Oral	<input type="checkbox"/> ポスター発表 Poster	言語 Language	<input type="checkbox"/> 日本語	<input type="checkbox"/> 英語 <input type="checkbox"/> 中国語
共同演者名 Co-presenter					

4. 受賞(研究業績) Award (Research achievement)

名称 Award name	国名 Country		受賞年 Year of award	年	月
	国名 Country		受賞年 Year of award	年	月

5. 本研究テーマに関わる他の研究助成金受給 Other research grants concerned with your research

受給実績 Receipt record	<input type="checkbox"/> 有 <input checked="" type="checkbox"/> 無
助成機関名称 Funding agency	
助成金名称 Grant name	
受給期間 Supported	年 月 ~ 年 月
受給額 Amount received	円
受給実績 Receipt record	<input type="checkbox"/> 有 <input checked="" type="checkbox"/> 無
助成機関名称 Funding agency	
助成金名称 Grant name	
受給期間 Supported	年 月 ~ 年 月
受給額 Amount received	円

6. 他の奨学金受給 Another awarded scholarship

受給実績 Receipt record	<input type="checkbox"/> 有 <input checked="" type="checkbox"/> 無
助成機関名称 Funding agency	
奨学金名称 Scholarship	
受給期間 Supported	年 月 ~ 年 月
受給額 Amount received	円

7. 研究活動に関する報道発表 Press release concerned with your research activities

※記載した記事を添付してください。 Attach a copy of the article described below

報道発表 Press release	<input type="checkbox"/> 有 <input checked="" type="checkbox"/> 無	発表年月日 Date of release	
発表機関 Released medium			
発表形式 Release method	・新聞 ・雑誌 ・Web site ・記者発表 ・その他 ()		
発表タイトル Released title			

8. 本研究テーマに関する特許出願予定 Patent application concerned with your research theme

出願予定 Scheduled	<input type="checkbox"/> 有 <input checked="" type="checkbox"/> 無	出願国 Application	
出願内容(概要) Application contents			

9. その他 Others

副論文(国をまたがる遠隔医療の法的リスクー中国在住患者に対する日本からの遠隔画像診断を中心にー)は2022年3月4日に国際医療福祉大学学会誌に投稿済み。
--

指導責任者(記名)

島崎謙治



日中笹川医学奨学金制度(学位取得コース)評価書

課程博士：指導教官用



第 42 期

研究者番号： G4210

作成日： 2022 年 3 月 8 日

氏 名	Zhai Da	翟 達	性別	F	生年月日	1992. 03. 12
所属機関（役職）	長崎大学大学院医歯薬学総合研究科放射線医療科学専攻幹細胞生物学（大学院生）					
研究先（指導教官）	長崎大学原爆後障害医療研究所幹細胞生物学研究分野（李 桃生教授）					
研究テーマ	メカノストレスが癌細胞に与える影響と機序 Effects and mechanisms of mechanical stresses on cancer cells					
専攻種別	<input type="checkbox"/> 論文博士			<input checked="" type="checkbox"/> 課程博士		

研究者評価（指導教官記入欄）

成績状況	優 良	取得単位数
		30/30
学生本人が行った研究の概要	悪性腫瘍組織内には様々なメカニカルストレスが高めている状態で、特に普遍的に存在している静水圧の上昇が癌細胞の生物学特性に与える影響が不明である。Zhai さんは静水圧が癌細胞に与える影響を In vitro と In vivo 実験で調べた。その結果、静水圧は癌細胞における HIF-1alpha 発現向上により、癌細胞の接着能と抗酸化能を強化され、転移し易くなったことが判明した。この研究成果は癌の治療と転移防止に貢献しうる。	
総合評価	【良かった点】 基本的なルールを守っており、研究室の皆さんととてもよい関係を保たれている。また、研究も一つの成果を出されて、論文と学会発表もできた。	
	【改善すべき点】 より貪欲的に新しいことを吸収、挑戦してほしい。	
	【今後の展望】 現在、「メカニカルストレスが癌幹細胞の性質転換における役割と機序解明」を新たな研究テーマとして進行中であり、よい研究成果を期待したい。	
学位取得見込	既に第一著者として原著論文が発表され、本大学の学位審査の規定により、博士(医学)学位授与の申請基準を満たしている。学位取得のためには、これまでの研究成果を纏めて、学位公開審査会の発表し、質疑応答にも合格できれば、2023 年 3 月に学位取得の見込みです。	
評価者（指導教官名）		李 桃生

日中笹川医学奨学金制度(学位取得コース)中間報告書 研究者用



第42期

研究者番号: G4210

作成日: 2022年3月8日

氏名	Zhai Da	翟 達	性別	F	生年月日	1992. 03. 12
所属機関(役職)	長崎大学大学院医歯薬学総合研究科放射線医療科学専攻幹細胞生物学(大学院生)					
研究先(指導教官)	長崎大学原爆後障害医療研究所幹細胞生物学研究分野(李 桃生教授)					
研究テーマ	メカノストレスが癌細胞に与える影響と機序 Effects and mechanisms of mechanical stresses on cancer cells					
専攻種別	論文博士		<input type="checkbox"/>	課程博士		<input checked="" type="checkbox"/>
<p>1. 研究概要(1)</p> <p>1) 目的(Goal)</p> <p>i. To investigate whether an elevated hydrostatic pressure in solid tumor promotes the metastasis of cancer cells. ii. To investigate whether an elevated hydrostatic pressure in solid tumor promotes the stemness of cancer cells. iii. To understand the relevant molecular mechanisms on tumor metastasis and stemness induced by elevated hydrostatic pressure.</p> <p>2) 戦略(Approach)</p> <p>Using a commercial device, we exposed Lewis lung cancer (LLC) cells to 50 mmHg for 24 hours, and then investigated the probable role of hydrostatic pressure on the metastatic property of LLC cells by in vitro and in vivo assessments. Using the same pressure device, we exposed human breast cancer cells to 50mmHg for 48 hours, and then investigated the probable role of hydrostatic pressure on the stemness of cancer cells.</p> <p>3) 材料と方法(Materials and methods)</p> <p>1. <i>Lewis lung carcinoma (LLC) cells and hydrostatic pressure stimulation</i> Lewis lung carcinoma (LLC) cells was used for experiments. A pneumatic pressurizing system (Strex. Inc.) was used for inducing 50mmHg hydrostatic pressure to LLC cells for 24h (HP group). The cells without hydrostatic pressure exposure were used as control (CON group).</p> <p>2. <i>Adhesion assay</i> The freshly harvested cells (5 x10⁴ cells in 5 ml DMEM) were seeded on 25 cm² Collagen I-coated Flask. After 60 minutes incubation, unattached cells were gently removed by twice washing with PBS. The number of adherent cells were counted under a microscope with 200-fold magnification.</p> <p>3. <i>Detection of HIF-1α and antioxidant enzymes expression</i> Use Western blot to detect the expression of HIF-1α, SOD1, SOD2 in LLC cells after hydrostatic pressure stimulation.</p> <p>4. <i>Evaluation on oxidative stress resistance</i> Cells were stimulated with 50uM, 20uM H₂O₂ and without H₂O₂ for 2 h. Cells were then labeled with ANNEXIN V-FITC and propidium iodide (PI) to detect the apoptosis and dead cells. Quantitative flow cytometry analysis was performed using a FACSCalibur.</p> <p>5. <i>Experimental lung cancer metastasis model</i> LLC cells (5x10⁵) cultured at 50mmHg or without hydrostatic pressure were injected intravenously to C57BL/6 mice (10 to 12-week-old). Lung tissues were excised and weighted at 4 weeks later, and the number of tumor nodule in lungs were counted.</p> <p>6. <i>Evaluation on ALDH activity and stemness markers</i> MCF-7 breast cancer cells were treated under 50mmHg for 48 hours and then were detected for ALDH activity and stemness markers expression.</p> <p>4) 実験結果(Results)</p> <p>1. <i>Hydrostatic pressure exposure enhanced the adhesion property of LLC cells.</i> There was not obvious difference in cell morphology and cell number after 24 hours exposure to 50mmHg hydrostatic pressure (Figure 1A). Adhesion property is critical for cancer cell metastasis. We found that the exposure to 50 mmHg hydrostatic pressure significantly increased the number of adherent cells on collagen I-coated flask (Figure 1B).</p> <p>2. <i>Hydrostatic pressure exposure increased the expression of HIF-1α and antioxidant enzymes in LLC cells.</i> HIF-1α is known to play critical roles in the metabolic reprogramming and metastasis of cancer cells. Western blotting showed that the expression of HIF-1α was significantly increased in the HP group (Figure 2A). We further investigated the expression of antioxidant enzymes of SOD1 and SOD2, which belongs to HIF-1α downstream signals. As expected, the exposure to 50 mmHg hydrostatic pressure for 24 hours also significantly upregulated the expression of SOD1 and SOD2 in LLC cells (Figure 2B, 2C).</p>						

1. 研究概要(2)

3. Hydrostatic pressure exposure induced the tolerance of LLC cells to oxidative stress.

As hydrostatic pressure showed to enhance the expression of SOD1 and SOD2, we evaluated the oxidative stress tolerance. The necrosis under 20 or 50 μ M H₂O₂ stimulation were significantly reduced in these LLC cells pretreated with 50 mmHg hydrostatic pressure for 24 hours, although the apoptotic cells were not significantly different between groups (Figure 3).

4. Hydrostatic pressure exposure promoted the metastasis of LLC cells to lungs.

To evaluate the metastatic potency in vivo, we intravenously injected LLC cells into healthy adult mice. Compared with the mice that received LLC cells without hydrostatic pressure exposure, significantly worse survival was observed in the mice that received LLC cells pretreated with 50 mmHg (Figure 4A). All mice were killed at 4 weeks after cell injection and we found significantly more metastatic tumor lesions in lungs of mice in the HP group than in the CON group (Figure 4B, 4C). The weights of lung tissues were also significantly higher in the HP group than in the CON group (Figure 4D).

5. Hydrostatic pressure increased ALDH activity of breast cancer cells.

To investigate how hydrostatic pressure affect the cancer cell stemness, we detect the cell ALDH activity level. We found that 50mmHg hydrostatic pressure treatment for 48 hours significantly increased the ALDH activity in the MCF-7 cells than the CON group (Figure 5).

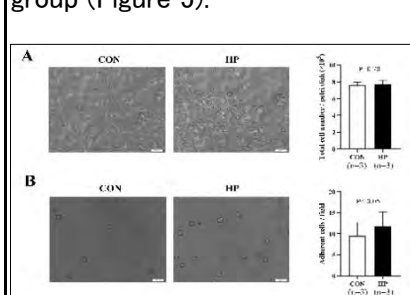


Figure 1

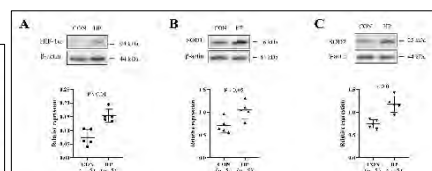


Figure 2

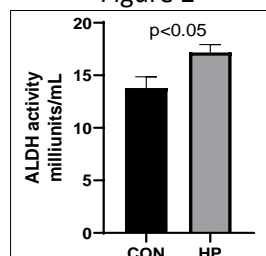


Figure 3

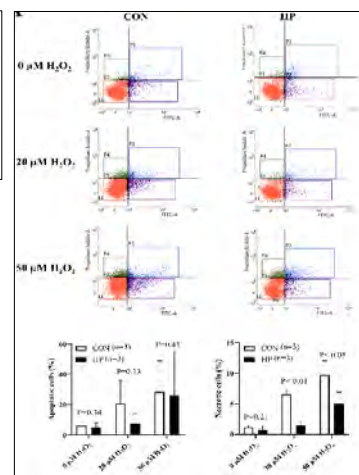


Figure 4

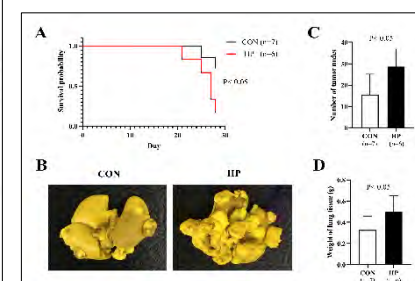


Figure 5

5) 考察 (Discussion)

Various mechanical forces within the microenvironment of tumor mass has been reported to play critical roles in the progression of malignant tumors [1]. Among the multiple mechanical forces, an elevated interstitial fluid hydrostatic pressure can be commonly induced by the presence of excess fluid due to the hyper-permeability of immature capillaries within malignant tumors [2]. Recent studies have reported that hydrostatic pressure may drive cancer cells toward more invasive phenotype [3], but precise role and mechanism of mechanical forces in metastasis have poorly been addressed.

To investigate the role of hydrostatic pressure on metastatic property of cancer cells, we exposed LLC cells to 50 mmHg hydrostatic pressure by mimicking the in vivo tumor microenvironment. Using an experimental lung metastasis model, we further confirmed that the pretreatment of LLC cells with 50 mmHg hydrostatic pressure resulted in significantly higher number of tumor nodes in lungs of mice. These data suggested that an elevated interstitial fluid hydrostatic pressure in rapid growing malignant tumors might enhance the metastatic property of cancer cells.

We then tried to further understand how hydrostatic pressure enhanced the metastatic property of LLC cells. It is known that cancer cells have to enter the circulation system and expose to the hyperoxic arterial blood for hematogenous metastasis [4]. Accumulating evidences have suggested that oxidative stress kills the most of circulating cancer cells [4]. Therefore, oxidative stress tolerance is essential for the successful metastasis of cancer cells. HIF-1 α has been well recognized as an important mediator on the metabolism reprogramming of cancer cells by regulating the antioxidant enzymes and antioxidant properties. Very interestingly, it has been recently demonstrated that cyclic mechanical force stabilizes HIF-1 α by reducing protein degradation [5]. Consistently, our data exactly showed a significant increase of HIF-1 α in LLC cells with 24 hours exposure to 50 mmHg hydrostatic pressure. Hydrostatic pressure exposure also significantly enhanced the expressions of SOD1 and SOD2, and induced the oxidative stress tolerance of LLCs cells.

Based on the data of this study, an elevated hydrostatic pressure in malignant tumor environment may enhance the metastatic potency of cancer cells, through the stabilization of HIF-1 α to induce the expression of antioxidant enzymes for defending against oxidative damage during metastasis.

6) 参考文献 (References)

- [1] Bregenzner ME, Horst EN, Mehta P, Novak CM, Repetto T, Mehta G. The role of cancer stem cells and mechanical forces in ovarian cancer metastasis. *Cancers*. 11 (2019) 1008.
- [2] Jain RK, Martin JD, Stylianopoulos T. The role of mechanical forces in tumor growth and therapy. *Annu Rev Biomed Eng*. 16 (2014) 321–346.
- [3] Tse JM, Cheng G, Tyrrell JA, et al. Mechanical compression drives cancer cells toward invasive phenotype. *Proc Natl Acad Sci U S A*. 109 (2012) 911–916.
- [4] Piskounova E, Agathocleous M, Murphy MM, et al. Oxidative stress inhibits distant metastasis by human melanoma cells. *Nature*. 527 (2015) 186–191.
- [5] Solis AG, Bielecki P, Steach HR, et al. Mechanosensation of cyclical force by PIEZO1 is essential for innate immunity. *Nature*. 573 (2019) 69–74.

2. 執筆論文 Publication of thesis ※記載した論文を添付してください。Attach all of the papers listed below.

論文名 1 Title	Hydrostatic pressure stabilizes HIF-1 α expression in cancer cells to protect against oxidative damage during metastasis					
掲載誌名 Published journal	Oncology Reports					
	2021 年 10 月	46 巻(号)	頁 ~	頁	言語 Language	English
第1著者名 First author	DA ZHAI	第2著者名 Second author	YONG XU		第3著者名 Third author	LINA ABDELGHANY
その他著者名 Other authors	XU ZHANG, JINGYAN LIANG, SHOUHUA ZHANG, CHANGYING GUO, TAO-SHENG LI					
論文名 2 Title	Nicaraven mitigates radiation-induced lung injury by downregulating the NF- κ B and TGF- β /Smad pathways to suppress the inflammatory response					
掲載誌名 Published journal	Journal of Radiation Research					
	2022 年 1 月	巻(号)	1 頁 ~	8 頁	言語 Language	English
第1著者名 First author	Yong Xu	第2著者名 Second author	Da Zhai		第3著者名 Third author	Shinji Goto
その他著者名 Other authors	Xu Zhang, Keiichi Jingu, Tao-Sheng Li					
論文名 3 Title	Biphasic effect of mechanical stress on lymphocyte activation					
掲載誌名 Published journal	Journal of Cellular Physiology					
	2022 年 2 月	237 巻(号)	1521 頁 ~	1531 頁	言語 Language	English
第1著者名 First author	Mhd Yousuf Yassouf	第2著者名 Second author	Xu Zhang		第3著者名 Third author	Zisheng Huang
その他著者名 Other authors	Da Zhai, Reiko Sekiya, Tsuyoshi Kawabata, Tao-Sheng Li					
論文名 4 Title						
掲載誌名 Published journal						
	年 月	巻(号)	頁 ~	頁	言語 Language	
第1著者名 First author		第2著者名 Second author			第3著者名 Third author	
その他著者名 Other authors						
論文名 5 Title						
掲載誌名 Published journal						
	年 月	巻(号)	頁 ~	頁	言語 Language	
第1著者名 First author		第2著者名 Second author			第3著者名 Third author	
その他著者名 Other authors						

3. 学会発表 Conference presentation ※筆頭演者として総会・国際学会を含む主な学会で発表したものを記載してください

※Describe your presentation as the principal presenter in major academic meetings including general meetings or international meetings

学会名 Conference	Japanese Cancer Association			
演題 Topic	Hydrostatic pressure stabilizes HIF-1 α of cancer cells to defense against oxidative damage during metastasis			
開催日 date	2020 年 10 月 1 日	開催地 venue	広島	
形式 method	<input checked="" type="checkbox"/> 口頭発表 Oral <input type="checkbox"/> ポスター発表 Poster	言語 Language	<input type="checkbox"/> 日本語 <input checked="" type="checkbox"/> 英語 <input type="checkbox"/> 中国語	
共同演者名 Co-presenter	Taosheng Li			
学会名 Conference				
演題 Topic				
開催日 date	年 月 日	開催地 venue		
形式 method	<input type="checkbox"/> 口頭発表 Oral <input type="checkbox"/> ポスター発表 Poster	言語 Language	<input type="checkbox"/> 日本語 <input type="checkbox"/> 英語 <input type="checkbox"/> 中国語	
共同演者名 Co-presenter				
学会名 Conference				
演題 Topic				
開催日 date	年 月 日	開催地 venue		
形式 method	<input type="checkbox"/> 口頭発表 Oral <input type="checkbox"/> ポスター発表 Poster	言語 Language	<input type="checkbox"/> 日本語 <input type="checkbox"/> 英語 <input type="checkbox"/> 中国語	
共同演者名 Co-presenter				
学会名 Conference				
演題 Topic				
開催日 date	年 月 日	開催地 venue		
形式 method	<input type="checkbox"/> 口頭発表 Oral <input type="checkbox"/> ポスター発表 Poster	言語 Language	<input type="checkbox"/> 日本語 <input type="checkbox"/> 英語 <input type="checkbox"/> 中国語	
共同演者名 Co-presenter				

4. 受賞(研究業績) Award (Research achievement)

名称 Award name	国名 Country		受賞年 Year of award	年 月
	国名 Country		受賞年 Year of award	年 月

5. 本研究テーマに関わる他の研究助成金受給 Other research grants concerned with your research theme

受給実績 Receipt record	<input type="checkbox"/> 有 <input checked="" type="checkbox"/> 無
助成機関名称 Funding agency	
助成金名称 Grant name	
受給期間 Supported period	年 月 ~ 年 月
受給額 Amount received	円
受給実績 Receipt record	<input type="checkbox"/> 有 <input type="checkbox"/> 無
助成機関名称 Funding agency	
助成金名称 Grant name	
受給期間 Supported period	年 月 ~ 年 月
受給額 Amount received	円

6. 他の奨学金受給 Another awarded scholarship

受給実績 Receipt record	<input type="checkbox"/> 有 <input checked="" type="checkbox"/> 無
助成機関名称 Funding agency	
奨学金名称 Scholarship name	
受給期間 Supported period	年 月 ~ 年 月
受給額 Amount received	円

7. 研究活動に関する報道発表 Press release concerned with your research activities

※記載した記事を添付してください。Attach a copy of the article described below

報道発表 Press release	<input type="checkbox"/> 有 <input checked="" type="checkbox"/> 無	発表年月日 Date of release	
発表機関 Released medium			
発表形式 Release method	・新聞 ・雑誌 ・Web site ・記者発表 ・その他()		
発表タイトル Released title			

8. 本研究テーマに関する特許出願予定 Patent application concerned with your research theme

出願予定 Scheduled application	<input type="checkbox"/> 有 <input checked="" type="checkbox"/> 無	出願国 Application	
出願内容(概要) Application contents			

9. その他 Others

--

指導責任者(署名)

李桃生

Hydrostatic pressure stabilizes HIF-1 α expression in cancer cells to protect against oxidative damage during metastasis

DA ZHAI^{1,2}, YONG XU^{1,2}, LINA ABDELGHANY^{1,2,3}, XU ZHANG^{1,2}, JINGYAN LIANG⁴,
SHOUHUA ZHANG⁵, CHANGYING GUO⁶ and TAO-SHENG LI^{1,2}

¹Department of Stem Cell Biology, Atomic Bomb Disease Institute, Nagasaki University; ²Department of Stem Cell Biology, Nagasaki University Graduate School of Biomedical Sciences, Nagasaki 852-8523, Japan; ³Department of Pharmacology and Toxicology, Faculty of Pharmacy, Tanta University, Tanta 31527, Egypt; ⁴Institute of Translational Medicine, Medical College, Yangzhou University, Yangzhou, Jiangsu 225000; ⁵Department of General Surgery, Jiangxi Provincial Children's Hospital; ⁶Department of Thoracic Surgery, Jiangxi Cancer Hospital, Nanchang, Jiangxi 330000, P.R. China

Received November 6, 2020; Accepted April 23, 2021

DOI: 10.3892/or.2021.8162

Abstract. The tissue microenvironment is known to play a pivotal role in cancer metastasis. Interstitial fluid hydrostatic pressure generally increases along with the rapid growth of malignant tumors. The aim of the present study was to investigate the role and relevant mechanism of elevated hydrostatic pressure in promoting the metastasis of cancer cells. Using a commercial device, Lewis lung cancer (LLC) cells were exposed to 50 mmHg hydrostatic pressure (HP) for 24 h. The survival time and morphology of the cells did not notably change; however, the results from a PCR array revealed the upregulation of numerous metastasis-promoting genes (*Hgf*, *Cdh11* and *Ephb2*) and the downregulation of metastasis suppressing genes (*Kiss1*, *Syk* and *Htatip2*). In addition, compared with that in the control, the cells which had undergone exposure to 50 mmHg HP showed significantly higher protein expression level of HIF-1 α and the antioxidant enzymes, SOD1 and SOD2, as well as improved tolerance to oxidative stress ($P < 0.05$ vs. control). Following an intravenous injection of the LLC cells into healthy mice, to induce lung metastasis, it was found that the exposure of the LLC cells to 50 mmHg HP for 24 h, prior to injection into the mice, resulted in higher cell survival/retention in the lungs 24 h later and also resulted in more metastatic tumor lesions 4 weeks later ($P < 0.05$ vs. control). Further investigation is required to confirm the molecular mechanism; however, the results from the present study suggested that elevated interstitial fluid HP in malignant tumors may promote the metastasis of cancer cells by stabilizing HIF-1 α expression to defend against oxidative damage.

Introduction

Metastasis occurs in ~90% of malignant tumors and is the leading cause of cancer-associated mortality in patients with cancer worldwide (1,2). A number of biological factors and multiple signaling pathways, such as epithelial-mesenchymal transition, resistance to apoptosis and angiogenesis have been associated with the complex processes of metastasis (3); however, a novel approach for effectively controlling tumor metastasis is still required.

Metastasis is defined as cancer cells leaving the original tumor mass and disseminating to other parts of the body via the bloodstream or lymphatic system. Therefore, the metastatic process represents a multi-step event (3). For example, remote hematogenous metastasis requires the cancer cells to successfully pass through the following steps: i) Transendothelial migration into the vessel (known as intravasation); ii) survival in the circulatory system; iii) attachment to the vessel wall and transendothelial migration out of the vessel (known as extravasation) and iv) eventually live and propagate at the distal site (4,5). All of these steps are accompanied with a change in the surrounding microenvironment, with various biomechanical forces and oxidative stress (6); therefore, metastasis can be a stressful and inefficient event to the cancer cell (7).

Biomechanical forces have been demonstrated to play critical roles in regulating cell migration and proliferation (8,9). With the rapid advancement of mechanobiology in recent years, it has become a hot topic for understanding how biomechanical forces mediate malignant tumor progression (2,8). Beyond the mechanical stress during metastatic processes, it is also well-known that elevated interstitial fluid hydrostatic pressure (HP) occurs in solid tumors (10,11). Higher interstitial fluid HP in tumor mass has been demonstrated to be associated with a worse prognosis in patients with head and neck cancer (12). Furthermore, the exposure of cancer cells to 20 mmHg HP has been demonstrated to accelerate cell motility (8). However, it is not clear whether and how the elevation of interstitial fluid HP in tumor mass promotes the metastasis of cancer cells.

Correspondence to: Professor Tao-Sheng Li, Department of Stem Cell Biology, Atomic Bomb Disease Institute, Nagasaki University, 1-12-4 Sakamoto, Nagasaki 852-8523, Japan
E-mail: litaoshe@nagasaki-u.ac.jp

Key words: hydrostatic pressure, HIF-1 α , metastasis, oxidative stress, adhesion

Notably, it has recently been reported that cyclical mechanical force can induce the stabilization of HIF-1 α and upregulate the protein expression level of CXCL2 in monocytes (13). HIF-1 α is well-known as a master upstream regulator of oxidative stress, metabolism and DNA repair of cells (14-16). Therefore, we hypothesized that elevated interstitial fluid HP in a rapid growing malignant tumor may stabilize HIF-1 α to promote the metastasis of cancer cells.

In the present study, mouse Lewis lung carcinoma (LLC) cells were exposed to 50 mmHg HP for 24 h, then the role of HP on the metastatic property of these cells was investigated using both *in vitro* and *in vivo* experiments.

Materials and methods

Cells and animals. The LLC cells (LL/2) were used for the experiments. The cells were maintained in DMEM (FUJIFILM Wako Pure Chemical Corporation), supplemented with 10% fetal bovine serum (Cytiva) and 1% penicillin/streptomycin (Gibco; Thermo Fisher Scientific, Inc.), and cultured at 37°C in a humidified incubator with 5% CO₂.

A total of 19, male C57BL/6 mice (10-12 weeks old; weight, 23-25 g; CLEA Japan, Inc.) were used for the *in vivo* study. The mice were kept in specific, pathogen-free conditions and were allowed free access to food and water under a controlled temperature (24±1°C) with 55% humidity in a 12-h light/dark cycle. The animal experiments were approved by the Institutional Animal Care and Use Committee of Nagasaki University (approval no. 1608251335-11). All the animal procedures were performed in accordance with institutional and national guidelines. At the end of the experiments, the mice were administered with general anesthesia using an intraperitoneal injection of mixed anesthetics (0.75 mg/kg medetomidine, 4 mg/kg midazolam and 5 mg/kg butorphanol) and sacrificed by severing the abdominal aorta for blood removal. The removal of vital organs (lung tissue) was used as confirmation of the death of the mice following sacrifice.

HP stimulation. HP was induced in the LLC cells using a pneumatic pressurizing system (Strex, Inc.). Briefly, the LLC cells were seeded in 60 mm diameter Petri dishes (1x10⁵ cells/dish) and cultured for 36 h to form an adherent monolayer. The culture dishes were then randomly selected to move into a sealed chamber in which 50 mmHg HP was stably applied using the pneumatic pressurizing system and kept for 24 h (HP group). The culture dishes without HP exposure were used as the control (CON group).

Cell morphology observation and cell count. Cell morphology was observed under a light microscope (IX71S8F-3; Olympus Corporation) at x200 magnification, 24 h following HP exposure. Then, the cells were collected as a single cell suspension to measure the total cell number using a TC20™ Automated Cell Counter (Bio-Rad Laboratories, Inc.).

Reverse transcription (RT)² Profiler™ PCR array. To investigate the mRNA expression level of genes associated with metastasis, RNA was isolated from the cells using a Quick-RNA™ MicroPrep kit (Zymo Research Corp.). The

concentration of RNA was measured using a NanoDrop® 2000 spectrophotometer (Thermo Fisher Scientific, Inc.). Then, 1 μ g RNA was used to generate cDNA using the RT² First Strand kit (Qiagen Corporation), at 25°C for 10 min, 42°C for 60 min, then 85°C for 5 min. Mouse Tumor Metastasis RT² Profiler™ PCR array (cat. no. 330231; Qiagen Corporation) was used with a RT² SYBR-Green Master mix, according to the manufacturer's instructions and a Roche LightCycler 480 machine (Roche Diagnostics). The array contained a total of 84 genes associated with metastasis. The genes included in the assay were also defined by biological function by the manufacturer. The fold change in expression to the control was calculated using a web-based data analysis program (<https://geneglobe.qiagen.com/jp/analyze>). Among the 5 available housekeeping genes (*Actb*, *B2m*, *Gapdh*, *Gusb* and *Hsp90ab1*) in the array, *Actb*, *Gusb* and *Hsp90ab1* were automatically selected as the optimal set of internal control for normalization.

Adhesion assay. To evaluate the adhesion ability, the cells from both the HP and CON groups were harvested as single cell suspensions. Freshly harvested cells (5x10⁴ cells in 5 ml DMEM) were seeded onto a 25-cm² Collagen I-coated Flask (Thermo Fisher Scientific, Inc.). Following incubation for 60 min, the unattached cells were gently removed by washing with PBS twice. The number of adherent cells was counted under a light microscope at x200 magnification. The average cell count from >20 randomly selected fields was used for statistical analysis.

Western blot analysis. The protein expression level of HIF-1 α , SOD1 and SOD2 was evaluated using western blot analysis, as previously described (17). Total protein from the cells was extracted using 1X RIPA buffer (FUJIFILM Wako Pure Chemical Corporation) and the concentration was detected using a BCA assay. A total of 30 μ g protein from each sample was separated using 10-12% SDS-PAGE, then transferred to 0.2- μ m PVDF membranes (Bio-Rad Laboratories, Inc.). After blocking with 5% skimmed milk for 1 h at room temperature, the membranes were incubated with primary antibodies against HIF-1 α (1:250 dilution; cat. no. ab1; room temperature for 2 h; Abcam), SOD1 (1:500 dilution; cat. no. sc11407; overnight at 4°C; Santa Cruz Biotechnology, Inc.), SOD2 (1:500 dilution; cat. no. sc30080; overnight at 4°C; Santa Cruz Biotechnology, Inc.) and β -actin (1:1,000 dilution; cat. no. 8457S; overnight at 4°C; Cell Signaling Technology, Inc.), followed by incubation with horseradish peroxidase-conjugated secondary antibodies (rabbit anti-mouse, 1:1,000 dilution; cat. no. P026002; goat anti-rabbit, 1:1,000 dilution; cat. no. P044801) (both from Dako; Agilent Technologies, Inc.) at room temperature for 1 h. The expression level was visualized using an enhanced chemiluminescence detection kit (Thermo Fisher Scientific, Inc.). Semi-quantitative analysis was done using ImageQuant LAS 4000 mini detection system (v1.0; GE Healthcare Life Sciences).

Evaluation of oxidative stress tolerance. To evaluate oxidative stress tolerance, the cells from both groups were treated with 0, 20 or 50 μ M hydrogen peroxide (H₂O₂) in PBS at 37°C for 2 h. The apoptotic cells were stained with Annexin V-FITC, while the necrotic cells were labelled with PI using an

Annexin V-FITC Apoptosis Detection Kit (Abcam). The cells without staining were used as negative control. Quantitative flow cytometry analysis was performed using a FACSVerse™ flow cytometer and analyzed using BD FACSuite Software (v1.2 Suite 1.0.2) (both from BD Biosciences).

In addition, intracellular reactive oxygen species (ROS) was detected in the cells. Briefly, the cells from both groups were treated with 0, 20 or 50 μM H_2O_2 in PBS at 37°C for 1 h, then incubated with 10 μM general oxidative stress indicator (CM-H2DCFDA; Invitrogen; Thermo Fisher Scientific, Inc.) for another 30 min in the dark. Cells without staining were used as a negative control. The accumulation of intracellular ROS was measured by fluorescence intensity using a FACSVerse™ flow cytometer (BD Biosciences) and analyzed using BD FACSuite Software (v1.2 Suite 1.0.2) (both from BD Biosciences).

Experimental lung cancer metastasis model. To evaluate the metastatic potency, experimental lung cancer metastasis was induced in mice using an intravenous injection of LLC cells (5×10^5 cells in 0.5 ml saline) from the HP (n=6) and the CON (n=7) groups. A total of 4 weeks after the cells were injected into the mice, all the mice were sacrificed as aforementioned. Removal of lung tissue was used for both confirmation of mice death and experimental evaluation. Excised lung tissue was weighed and the number of tumor lesions on the lung surface was counted. For the mice that spontaneously died during the 4-week follow-up period, the date of death was recorded and the lung tissue samples were collected for evaluation. Statistical analysis of the overall survival rate of the mice was also determined.

Immunohistochemical staining. The cell proliferation and microvessel density in the metastatic lesions of the lungs was detected using immunohistochemistry staining. The lungs were fixed in 4% paraformaldehyde for 24 h, at 4°C, and paraffin-embedded sections (6- μm thick) were deparaffinized and rehydrated (xylene, 2x3 min washes; xylene 1:1 with 100% ethanol, 3 min; 100% ethanol, 2x3 min washes; 95% ethanol, 3 min; 70% ethanol, 3 min; 50% ethanol, 3 min; running cold tap water to rinse). After blocking with 1% BSA in PBS (Sigma-Aldrich; Merck KGaA), the sections were incubated with rabbit anti-mouse Ki67 antibody (cat. no. ab16667; 1:100 dilution;) and rabbit anti-mouse CD31 antibody (cat. no. ab28394; 1:150 dilution) (both from Abcam) overnight at 4°C, followed by incubation with the Alexa fluorescent 546-conjugated goat anti rabbit IgG(H+L) secondary antibody (cat. no. A11013; 1:350 dilution; Invitrogen; Thermo Fisher Scientific, Inc.) at room temperature for 1 h. Nuclei were stained with 4, 6-diamidino-2-phenylindole (DAPI; cat. no. D21490; Thermo Fisher Scientific, Inc.) at room temperature for 5 min. Positive staining was examined under a fluorescent microscope (FV10C-W3; Olympus Corporation). The percentage of Ki67-positive cells was calculated from 10 randomly selected fields of view (5 fields/slide in 2 slides) and used for statistical analysis. The CD31-positive stained structures were counted as microvessels and the average number of microvessels counted from 10 randomly selected fields of view (5 fields/slide in 2 slides) was used for statistical analysis.

PKH26 red fluorescent cell labeling. To evaluate the survival/retention of the LLC cells in the lungs of the mice, the cells were labelled with a PKH26 Red Fluorescent Cell Linker kit (Sigma-Aldrich; Merck KGaA). Briefly, the cells were incubated with 2 μM PKH26 dye for 5 min at room temperature, as the manufacturer's recommendations. Then, the mice were intravenously injected with the PKH26-labelled cells (1×10^6 cells in 0.5 ml saline) from the HP (n=3) and the CON (n=3) groups. The mice were sacrificed 24 h following the injection and the lung tissue samples were collected. Cryosections (8- μm thick) of the lung tissues were used for the direct detection of PKH26-labelled LLC cells under a fluorescent microscope (FV10C-W3; Olympus Corporation).

Statistical analysis. The data are presented as the mean \pm SD. Statistical significance between two groups was determined using an unpaired t-test (SPSS; v20.0; IBM Corp.). The survival of the mice was analyzed using a Kaplan-Meier curve and statistical significance was determined using the log-rank test (GraphPad Prism; v8.0.1; GraphPad Software, Inc.). $P < 0.05$ was used to indicate a statistically significant difference.

Results

Exposure of the LLC cells to 50 mmHg HP altered the mRNA expression level of numerous genes associated with metastasis. Firstly, the mRNA expression level of genes associated with metastasis was analyzed between the HP and CON groups. The RT² Profiler™ PCR array revealed that numerous genes were up- or downregulated, with a >1.3-fold difference in the HP group compared with that in the CON group (Table SI). The top 10 up- or downregulated genes are shown in Fig. 1A. Within the top 10 upregulated genes, the upregulation of several adhesion molecules was found, including *Cdh1*, *Cdh11* and *Fnl1* (Fig. 1B). In addition, the upregulation of numerous metastasis-promoting genes, such as *Hgf*, *Cdh11* and *Ephb2*, was also found. Within the top 10 downregulated genes, metastasis suppressors, including *Kiss1*, *Syk* and *Htatip2*, were frequently detected (Fig. 1B). The overall change in the gene expression profile indicated the potential role of HP in enhancing metastatic properties of the LLC cells.

HP exposure enhances the adhesion property of the LLC cells. The exposure of the LLC cells to 50 mmHg HP for 24 h did not induce notable morphological changes (Fig. 2A). The total number of harvested cells was also comparable between the groups ($P=0.70$; Fig. 2A), indicating a limited effect of 50 mmHg HP exposure on cell growth.

As the PCR array data indicated the upregulation of numerous adhesion molecules, the adhesion property of the cells was investigated. It was found that the exposure to 50 mmHg HP significantly increased the number of adherent cells on a collagen I-coated flask ($P < 0.05$; Fig. 2B).

HP exposure increases the protein expression level of HIF-1 α and antioxidant enzymes in the LLC cells. HIF-1 α , a master regulator of the cellular adaptive response to hypoxia, is known to play critical roles in metabolic reprogramming (16) and metastasis (14) in cancer cells. Western blot analysis showed

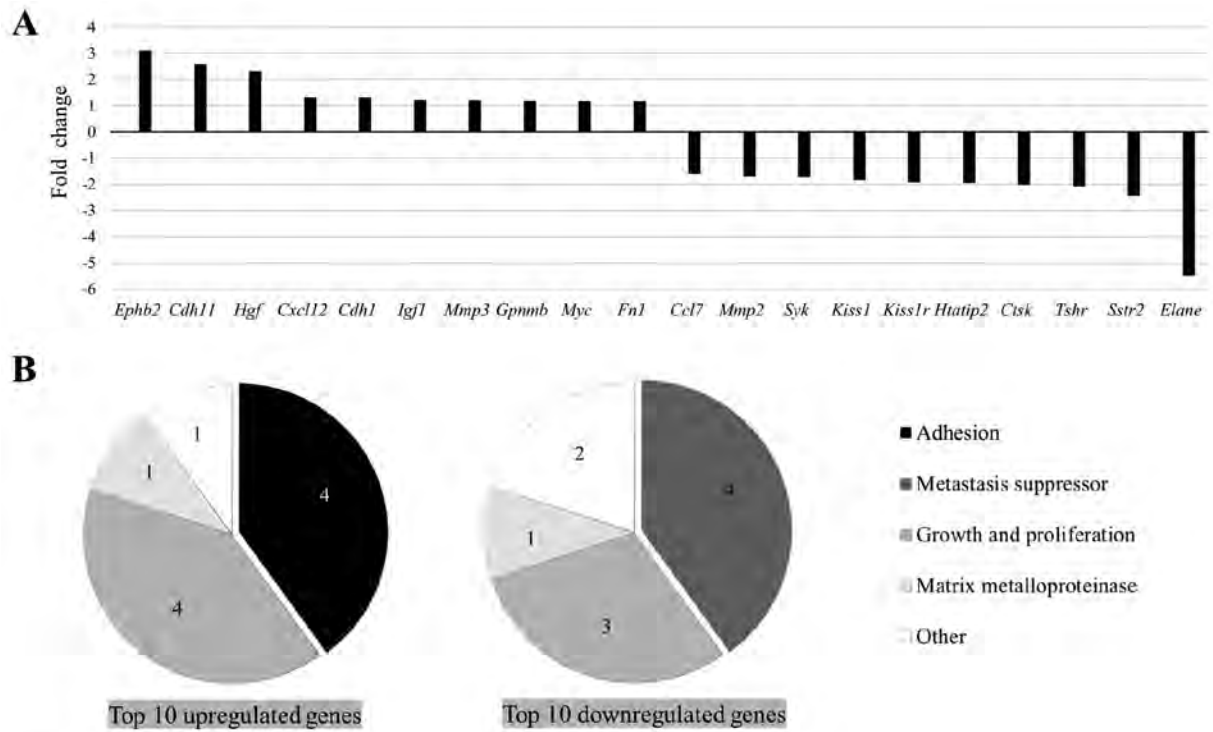


Figure 1. Change in the mRNA expression level of genes in the Lewis lung cancer cells following treatment with or without 50 mmHg HP for 24 h. The mRNA expression level of metastasis-related genes was measured using a reverse transcription² Profiler™ PCR array. The data are presented as the fold change in the cells with HP compared with that in the CON. The top 10 up- and downregulated genes are according to the (A) fold change and (B) the biological functional categories of the genes. HP, hydrostatic pressure exposure; CON, control.

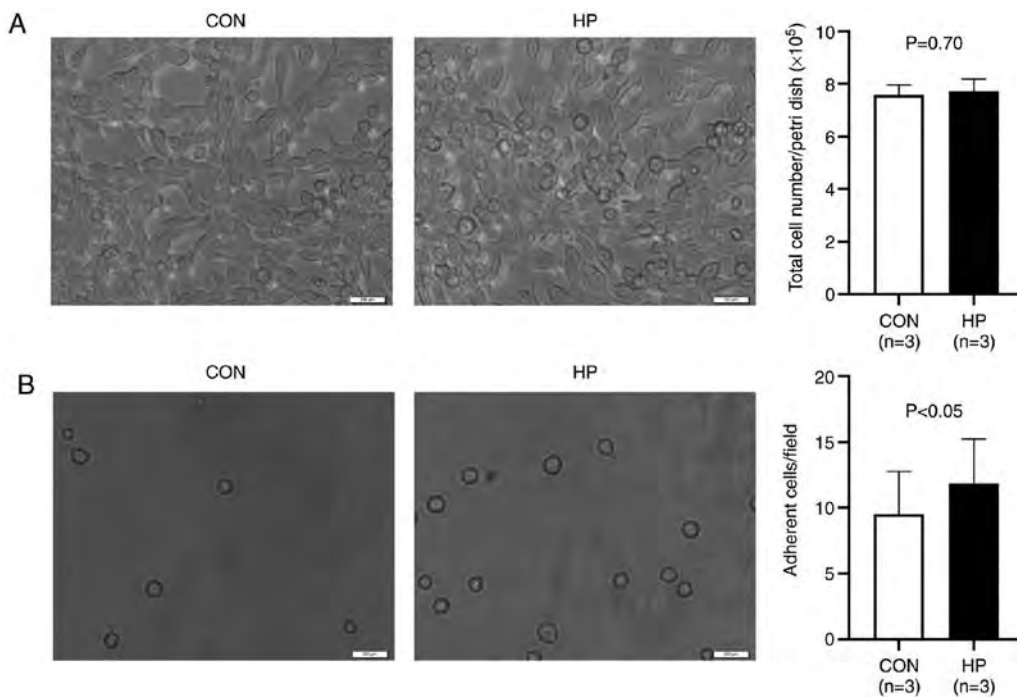


Figure 2. Survival and adhesion property of the Lewis lung cancer cells following treatment with or without 50 mmHg HP for 24 h. (A) Representative images of cell morphology under a phase-contrast microscope (left) and quantitative analysis of the total number of surviving cells per petri dish (right). (B) Representative images (left) and quantitative data (right) of the adherent cells in collagen I-coated flasks. Scale bar, 200 μ m. The data are presented as the mean \pm SD from 3 independent experiments. HP, hydrostatic pressure exposure; CON, control.

that the protein expression level of HIF-1 α was significantly increased in cells exposed to 50 mmHg HP for 24 h ($P<0.01$; Fig. 3A).

The protein expression level of the antioxidant enzymes, SOD1 and SOD2, which are HIF-1 α downstream signals (18,19), was also investigated. As expected, the exposure

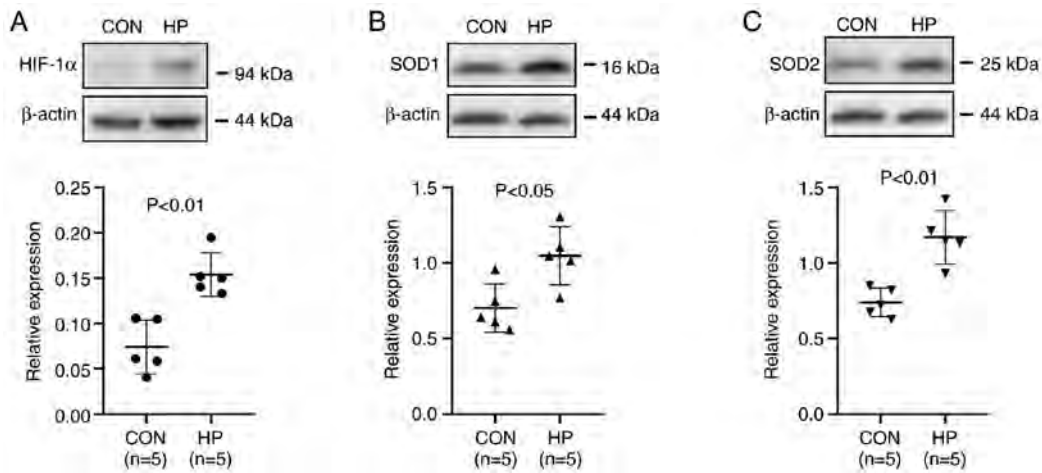


Figure 3. Protein expression level of HIF-1 α , SOD1 and SOD2 is increased following exposure of the LLC cells to 50 mmHg HP for 24 h. Representative blots and semi-quantitative analysis of the protein expression level of (A) HIF-1 α , (B) SOD1 and (C) SOD2 in the LLC cells following treatment with or without 50 mmHg HP for 24 h. The data are presented as the mean \pm SD from 5 independent experiments. HP, hydrostatic pressure; CON, control; LLC, Lewis lung cancer.

of the cells to 50 mmHg HP for 24 h also significantly upregulated the protein expression level of SOD1 and SOD2 ($P < 0.05$; Fig. 3B and C).

HP exposure induces the tolerance of the LLC cells to oxidative stress. In addition, the oxidative stress tolerance of the cells was investigated *in vitro*. Cell necrosis, under 20 or 50 μ M H₂O₂ treatment was significantly reduced in the LLC cells pretreated with 50 mmHg for 24 h ($P < 0.05$; Fig. 4A); however, the percentage of apoptotic cells was not significantly different between the 2 groups treated with 20 or 50 μ M H₂O₂ ($P = 0.26$ and $P = 0.45$, respectively; Fig. 4A).

The intracellular ROS level at the baseline (without H₂O₂ stimulation) was detected at comparable levels between the HP and CON groups (Fig. 4B). Unexpectedly, 1-h stimulation with 20 or 50 μ M H₂O₂ notably decreased the ROS accumulation in the LLC cells without pretreatment with 50 mmHg HP compared with that at baseline (Fig. 4B). By contrast, after 1-h stimulation with 20 μ M H₂O₂, the ROS accumulation was slightly increased in the LLC cells pretreated with 50 mmHg HP compared with that at baseline. We hypothesized that the less intracellular ROS accumulation in the LLC cells without HP exposure was due to the severe cell damage or cell death, rather than the resistance to oxidative stress.

HP exposure promotes the metastasis of the LLC cells to the lungs. To evaluate the metastatic potency *in vivo*, the LLC cells were intravenously injected into healthy adult mice. Compared with that in the mice that received LLC cells without HP exposure, significantly worse survival was observed in the mice that received LLC cells pretreated with 50 mmHg HP ($P < 0.05$; Fig. 5A). All the mice were killed 4 weeks following the injection of the cells and the maximum percentage body weight loss observed was 9.3%. There were significantly more metastatic tumor lesions in the lungs of the mice in the HP group compared with that in the CON group ($P < 0.05$; Fig. 5B and C). The weight of the lung tissue was also significantly higher in the HP group compared with that in the CON group ($P < 0.05$; Fig. 5D). These data suggested that HP exposure promoted the metastasis of the LLC cells to the lungs.

To further understand the mechanism involved, the LLC cells were labelled with PKH26 before intravenous injection into the mice, then the survival/retention of the cells in the lungs was analyzed 24 h later. As expected, more LLC cells (or cell clusters) were detected in the lungs from mice in the HP group compared with that in the CON group (Fig. 6A), suggesting an improved survival/retention of the LLC cells by pretreatment with 50 mmHg HP.

Cell proliferation and neovascularization in the metastatic lesions was also analyzed using immunostaining. The percentage of Ki67-positive cells was not significantly different between the HP and CON groups ($P = 0.20$; Fig. 6B). However, the density of the CD31-positive microvessels in the metastatic lesions was significantly higher in the HP group compared with that in the CON group ($P < 0.05$; Fig. 6C).

Discussion

Various mechanical forces within the microenvironment of the tumor mass have been reported to play critical roles in the progression of malignant tumors (2). Owing to the hyper-permeability of immature capillaries, the elevation of the interstitial fluid HP could be commonly induced by the presence of excess fluid accumulation within malignant tumors (20,21). A previous study has reported that HP may drive breast cancer cells toward a more invasive phenotype (9); however, the precise role and relevant mechanism of the mechanical forces in mediating metastasis is still not well understood.

To investigate the role of HP on the metastatic property of cancer cells, the LLC cells were exposed to 50 mmHg HP to mimic the *in vivo* tumor microenvironment, then the mRNA expression level of genes associated with tumor metastasis was analyzed. A PCR array indicated noticeable changes, including the upregulation of metastasis promoters (*Hgf*, *Cdh11* and *Ephb2*) and the downregulation of metastasis suppressors (*Kiss1*, *Syk* and *Htatip2*) in the LLC cells following exposure to 50 mmHg HP for 24 h. The most upregulated gene, *Ephb2*, has been demonstrated to modulate the metastatic phenotype (22) and induce angiogenesis (23). The most down-regulated gene, *Elane*, has been demonstrated to modulate

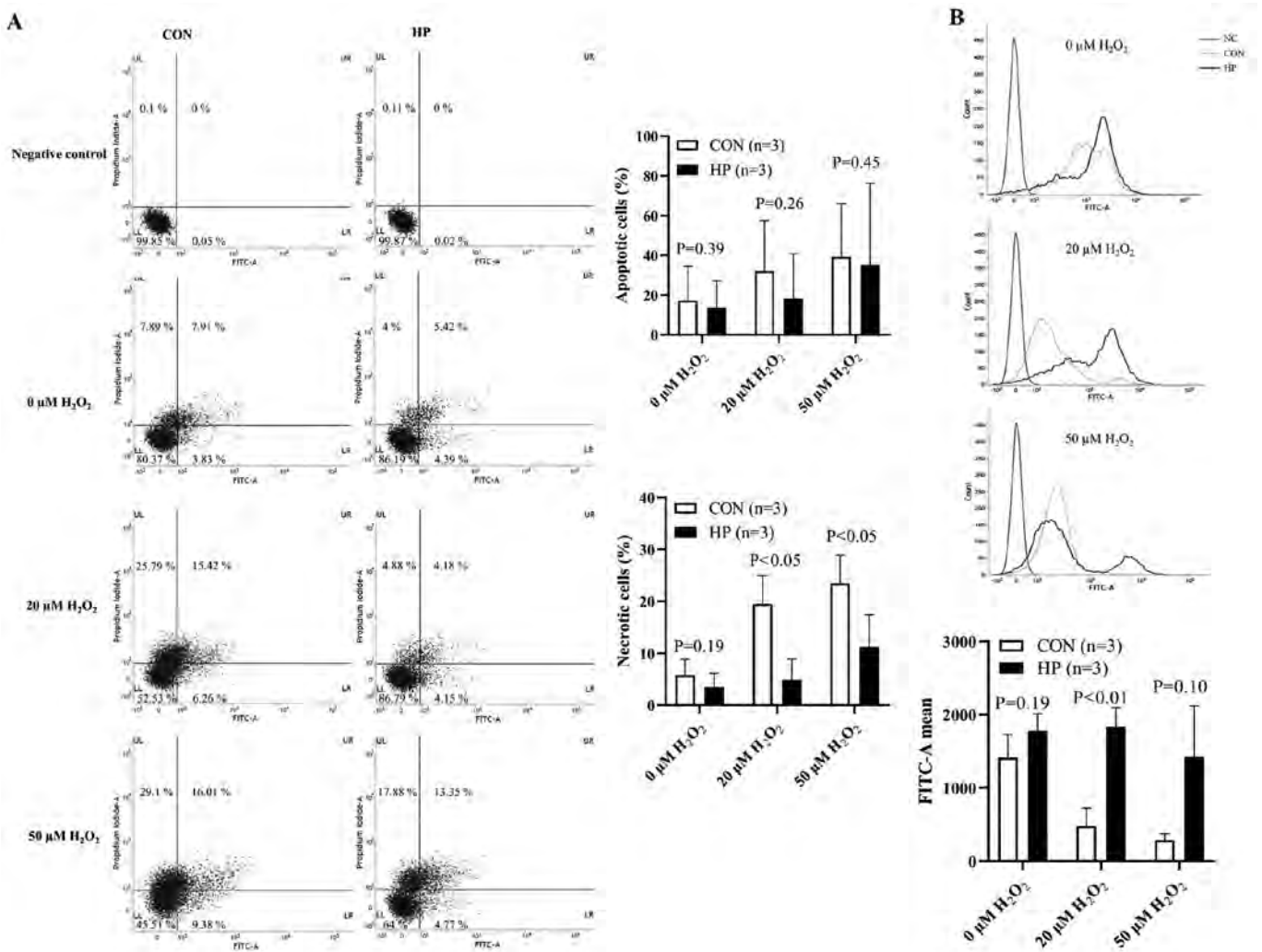


Figure 4. Tolerance of the LLC cells to oxidative stress. The LLC cells were treated with or without 50 mmHg HP and with 0, 20 and 50 μM H_2O_2 . The apoptotic/necrotic cells and intracellular ROS was subsequently detected using flow cytometry. (A) Representative flow cytometry plots (left) and quantitative data (right) of the number of apoptotic and necrotic cells. (B) Representative histograms (upper) and quantitative data (lower) of the mean intensity of the intracellular ROS levels. The data are presented as the mean \pm SD from three independent experiments. HP, hydrostatic pressure; CON, control; LLC, Lewis lung cancer; ROS, reactive oxygen species; H_2O_2 , hydrogen peroxide.

neutrophil expression, inflammation and repair (24). Using an experimental lung metastasis model in mice, it was further confirmed that the LLC cells pretreated with 50 mmHg HP developed a significantly higher number of tumor metastasis lesions in the lungs. These data suggested that an elevated interstitial fluid HP in a rapidly growing malignant tumor may enhance the metastatic property of cancer cells.

Additional experiments were performed to further understand how HP enhanced the metastatic property of the LLC cells from different aspects, according to the multi-step processes of hematogenous metastasis. It is well-known that cancer cells enter the circulation system and are exposed to hyperoxic arterial blood for hematogenous metastasis (6). Accumulating evidence suggests that oxidative stress kills most of the circulating cancer cells, resulting in a very poor efficiency of metastasis (6,7). Therefore, oxidative stress tolerance is essential for the successful metastasis of cancer cells. HIF-1 α is well-known as an important mediator of metabolism reprogramming of cancer cells by regulating antioxidant enzymes and antioxidant properties (25). Notably, it has been recently demonstrated that cyclic mechanical force stabilizes HIF-1 α by reducing protein

degradation (13). Consistently, the results from the present study showed the upregulation of HIF-1 α protein expression level in the LLC cells following exposure to 50 mmHg HP for 24 h. In addition, the protein expression level of the antioxidant enzymes, SOD1 and SOD2, the direct downstream targets of HIF-1 α (18,19), were also significantly increased in cells exposed to 50 mmHg HP. This could contribute to enhancing antioxidant capacity of cancer cells for remote hematogenous metastasis. Consistent with the upregulation of various adhesion molecules, the exposure to 50 mmHg HP also enhanced the adhesion property of the LLC cells, as shown by the results of the *in vitro* adhesion and the *in vivo* cell tracking assays.

HIFs are heterodimeric proteins composed of HIF- α and HIF-1 β subunits. HIF-1 α is an O_2 -regulated subunit, while HIF-1 β is a constitutively expressed subunit (26). The protein expression level of HIF-1 α has been reported to be overexpressed in numerous malignant tumors, including lung, prostate, breast and colon carcinomas (27,28). It has been demonstrated that the enhanced protein expression level of HIF-1 α was associated with poor prognosis in patients with breast, oropharyngeal and prostate cancer (29-31). As a master regulator of cellular response

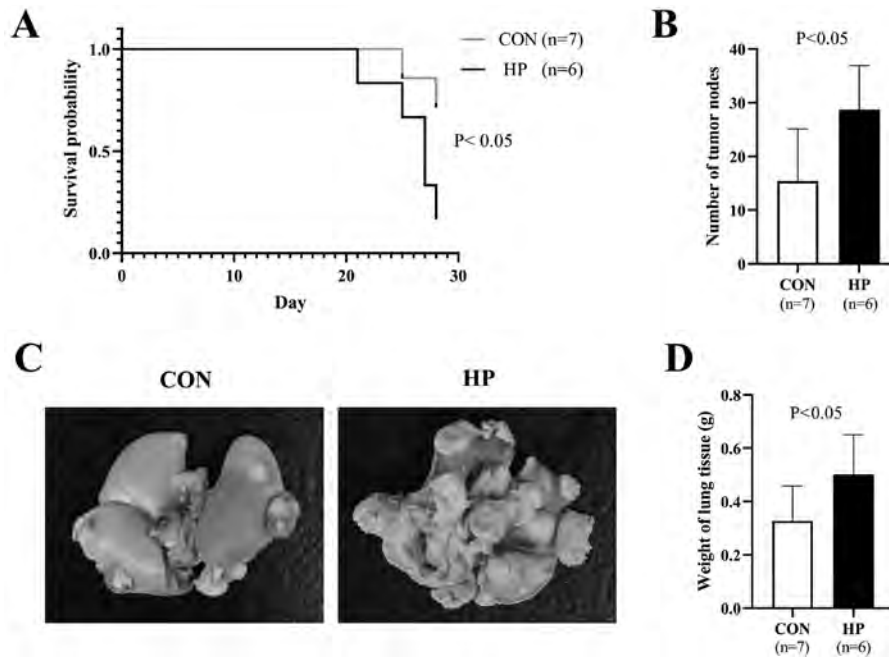


Figure 5. Experimental lung metastasis model in healthy adult mice. The Lewis lung cancer cells were treated with or without 50 mmHg HP and were intravenously injected into the mice, then lung metastasis was evaluated 4 weeks later. (A) Kaplan-Meier curves show the survival probability of the mice. (B) Quantitative data and (C) representative images of tumor metastasis lesions on the surface of lungs. (D) The weight of lung tissues. The data are presented as the mean \pm SD. HP, hydrostatic pressure; CON, control.

to hypoxia, HIF-1 can induce the transcription of several genes involved in angiogenesis, cell proliferation and cell metabolism (15,32). One of the most popularly recognized downstream genes of HIF-1 is vascular endothelial growth factor (VEGF), which is known to induce angiogenesis for the rapid growth of malignant tumors (33). VEGF, originally named as vascular permeability factor, was first identified as a tumor-secreted factor, which increases vascular permeability and promotes the accumulation of ascite fluid (21). Considering the hyper-permeability of microvessels in the tumor (34), it is reasonable to hypothesize that an excess accumulation of exudate in the interstitial space contributes, at least in part, to the increase of the interstitial fluid HP in the tumor mass. As a result, elevated HP may stabilize HIF-1 α , which thereby induces VEGF and antioxidant enzymes to accelerate the growth and metastasis of malignant tumors.

There is a caution in Cellosaurus that the LLC cells (LL/2) could be identical to 3LL cells. It is reported that LL/2 cell line could be identical to 3LL cell line because both of them are from mouse Lewis lung carcinoma and show the same biological characteristics. Therefore, this will not affect the conclusion of the present study.

A total of 4 weeks after the cells were injected into the mice was used as the humane endpoint, based on clinical signs (reduced intake and activity) and pathophysiological changes (weight loss >20%). During the follow-up for 4 weeks, the progression of tumor metastasis in the lungs of the mice was not directly monitored; however, it was indirectly monitored by observing the clinical signs (intake and activity) and pathophysiological changes (weight loss) of mice.

For the 7 mice that died spontaneously, prior to the end of the 4-week follow-up time in the lung metastasis mice model, it was confirmed that the 7 mice did not die from lung metastasis-induced respiratory failure or systemic cachexia.

We hypothesized that the cause of spontaneous death may be due to another cause, based on the following: i) There were no signs of severe clinical symptoms in the 7 mice following daily monitoring; ii) based on the assessment of the exercised lungs, there were fewer metastatic lesions in the lungs of the 7 mice; iii) according to the examination of the 7 mice after sacrifice, there was no serious bleeding, inflammation or purulent secretions in the body, no notable signs of metastasis or organ necrosis was found in the chest cavity or in any of the other organs and no obvious occurrence of cachexia was found.

The present study has several limitations. First, a single cell line was used and the cells were only exposed to 50 mmHg HP for all the experiments. This is due to the following reasons: i) The present study was designed to examine whether an elevated HP could promote the metastasis of cancer cells; ii) the C57BL/6 mice were used for *in vivo* experiments and the LLC cell line is the most reproducible syngeneic model for evaluating lung metastasis to date (35); iii) interstitial fluid pressure in solid malignant tumors could be elevated to ~30 mmHg HP (12,36) and iv) the exposure of the LLC cells to 50 mmHg HP altered the mRNA expression level of genes associated with metastasis; however, higher pressure (100 mmHg) induced cell death and cell debris production (data not shown). Therefore, further experiments are required to exposure different cancer cell lines with different HPs. Second, the PCR array was not repeated due to a limited budget. In addition, the fold-change result may also have greater variations if P>0.05; therefore, it is important to have a sufficient number of biological replicates to validate the array data. However, a mixture of RNA samples was used from three independent experiments to generate the cDNA for a single PCR array in each group. Therefore, the PCR array data was expressed as the average level in 3 samples from each group. Third, further interventional experiments, such as the interference of the HIF-1 α signaling

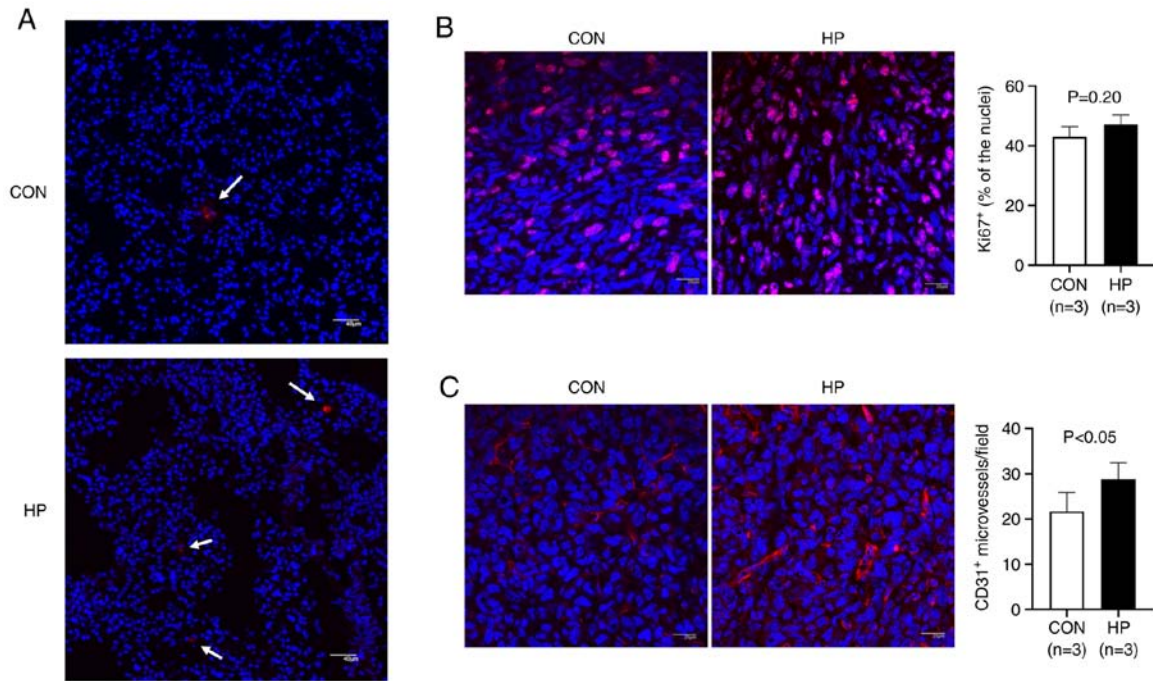


Figure 6. Survival/retention of the LLC cells and immunostaining analysis of proliferating cells and microvessels in the metastatic lesions. The LLC cells were treated with or without 50 mmHg HP, then intravenously injected into the mice. (A) Representative confocal microscopy images of the survival/retention of the PKH26-labelled cells or cell clusters (arrows) in the lungs, 24 h following injection. Scale bar, 40 μ m. (B) Representative images (left) and quantitative data (right) of the Ki67-positive proliferative cells in the metastatic lesions in lungs. Scale bar, 20 μ m. (C) Representative images (left) and quantitative data (right) of the CD31-positive microvessels in the metastatic lesions in the lungs. Scale bar, 20 μ m. The nuclei were stained with DAPI. The data are presented as the mean \pm SD. HP, hydrostatic pressure; CON, control; LLC, Lewis lung cancer.

pathway was not performed, as silencing HIF-1 α alone would change cell biological properties. Furthermore, multiple factors, including the increase in mRNA expression level of HIF-1 α and adhesion molecules could be involved in the HP-induced cancer cell metastasis; therefore, a genetic intervention approach to directly confirm the role of HIF-1 α was not performed in the present study. Forth, Annexin V-positive apoptotic cells were only analyzed using flow cytometry and the expression level of other apoptotic proteins, such as the caspase family, can also be used to indicate apoptosis. In addition, a colony-forming assay was not included, as the potential role of HP in cancer cell metastasis, rather than tumorigenesis and tumor growth was the aim of the present study.

From the results in the present study, an elevated HP in rapidly growing malignant tumors may enhance the metastatic potency of cancer cells via complex mechanisms, including the increase in the mRNA expression level of adhesion molecules to improve cell adhesion and the stabilization of HIF-1 α to induce the expression of antioxidant enzymes to defend against oxidative damage during metastasis (Fig. 7). It is critical to elucidate the comprehensive molecular mechanisms underlying the stabilization of HIF-1 α by HP in further investigations.

Acknowledgements

Not applicable.

Funding

This study was supported in part by a Grant-in-Aid from the Ministry of Education, Science, Sports, Culture and

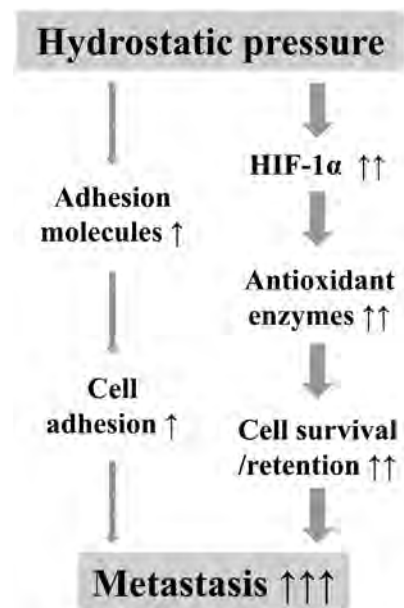


Figure 7. Schematic diagram of hydrostatic pressure induced metastasis of cancer cells. An elevated hydrostatic pressure in malignant tumors may enhance the metastatic potency of cancer cells by i) increasing the mRNA expression level of adhesion molecules to improve cell adhesion, and ii) stabilizing HIF-1 α to induce the expression of antioxidant enzymes to protect against oxidative damage.

Technology, Japan (grant no. 17H04265), the Collaborative Research Program of the Atomic-bomb Disease Institute of Nagasaki University and the Japan China Sasakawa Medical Fellowship.

Availability of data and materials

The datasets used and/or analyzed during the current study are available from the corresponding author on reasonable request.

Author's contributions

All the authors contributed to the conception and design of the study. DZ, YX and LA performed the experiments and acquired the data. TSL, DZ, YX, LA and XZ analyzed and interpreted the data. DZ and SZ drafted the manuscript. TSL, JL and CG critically revised the manuscript for important intellectual content. TSL and DZ confirmed the authenticity of all the raw data. All authors read and approved the final version of the manuscript.

Ethics approval and consent to participate

The animal experiments were approved by the Institutional Animal Care and Use Committee of Nagasaki University (approval no. 1608251335-11) and all animal procedures were performed in accordance with institutional and national guidelines.

Patient consent for publication

Not applicable.

Competing interests

The authors declare that they have no competing interests.

References

- Brabletz T, Lyden D, Steeg PS and Werb Z: Roadblocks to translational advances on metastasis research. *Nat Med* 19: 1104-1109, 2013.
- Bregenzler ME, Horst EN, Mehta P, Novak CM, Repetto T and Mehta G: The role of cancer stem cells and mechanical forces in ovarian cancer metastasis. *Cancers* 11: 1008, 2019.
- Eccles SA and Welch DR: Metastasis: Recent discoveries and novel treatment strategies. *Lancet* 369: 1742-1757, 2007.
- Fidler IJ: The pathogenesis of cancer metastasis: The 'seed and soil' hypothesis revisited. *Nat Rev Cancer* 3: 453-458, 2003.
- Zijl FV, Krupitza G and Mikulits W: Initial steps of metastasis: Cell invasion and endothelial transmigration. *Mutat Res* 728: 23-34, 2011.
- Piskounova E, Agathocleous M, Murphy MM, Hu Z, Huddleston SE, Zhao Z, Leitch AM, Johnson TM, DeBerardinis RJ and Morrison SJ: Oxidative stress inhibits distant metastasis by human melanoma cells. *Nature* 527: 186-191, 2015.
- Vanharanta S and Massague J: Origins of metastatic traits. *Cancer Cell* 24: 410-421, 2013.
- Kao YC, Jheng JR, Pan HJ, Liao WY, Lee CH and Kuo PL: Elevated hydrostatic pressure enhances the motility and enlarges the size of the lung cancer cells through aquaporin upregulation mediated by caveolin-1 and ERK1/2 signaling. *Oncogene* 36: 863-874, 2017.
- Tse JM, Cheng G, Tyrrell JA, Wilcox-Adelman SA, Boucher Y, Jain RK and Munn LL: Mechanical compression drives cancer cells toward invasive phenotype. *Proc Natl Acad Sci USA* 109: 911-916, 2012.
- Less JR, Posner MC, Boucher Y, Borochovitz D, Wolmark N and Jain RK: Interstitial hypertension in human breast and colorectal tumors. *Cancer Res* 52: 6371-6374, 1992.
- Nathan SS, DiResta GR, Casas-Ganem JE, Hoang BH, Sowers R, Yang R, Huvos AG, Gorlick R and Healey JH: Elevated physiologic tumor pressure promotes proliferation and chemosensitivity in human osteosarcoma. *Clin Cancer Res* 11: 2389-2397, 2005.
- Gutmann R, Leunig M, Feyh J, Goetz AE, Messmer K, Kastanbauer E and Jain RK: Interstitial hypertension in head and neck tumors in patients: Correlation with tumor size. *Cancer Res* 52: 1993-1995, 1992.
- Solis AG, Bielecki P, Steach HR, Sharma L, Harman CC, Yun S, de Zoete MR, Warnock JN, To SDF, York AG, *et al*: Mechanosensation of cyclical force by PIEZO1 is essential for innate immunity. *Nature* 573: 69-74, 2019.
- Rankin EB, Nam JM and Giaccia AJ: Hypoxia: Signaling the metastatic cascade. *Trends Cancer* 2: 295-304, 2016.
- Semenza GL: Hypoxia-inducible factors in physiology and medicine. *Cell* 148: 399-408, 2012.
- Semenza GL: Regulation of cancer cell metabolism by hypoxia-inducible factor 1. *Semin Cancer Biol* 19: 12-16, 2009.
- Urata Y, Goto S, Luo L, Doi H, Kitajima Y, Masuda S, Ono Y and Li TS: Enhanced Nox1 expression and oxidative stress resistance in c-kit-positive hematopoietic stem/progenitor cells. *Biochem Biophys Res Commun* 454: 376-380, 2014.
- Hu XQ, Song R and Zhang L: Effect of oxidative stress on the estrogen-NOS-NO-KCa channel pathway in uteroplacental dysfunction: Its implication in pregnancy complications. *Oxid Med Cell Longev* 2019: 9194269, 2019.
- Novak S, Drenjancevic I, Vukovic R, Kellermayer Z, Cosic A, Tolusic Levak M, Balogh P, Culo F and Mihalj M: Anti-inflammatory effects of hyperbaric oxygenation during DSS-induced colitis in BALB/c mice include changes in gene expression of HIF-1 α , proinflammatory cytokines, and antioxidative enzymes. *Mediators Inflamm* 2016: 7141430, 2016.
- Jain RK, Martin JD and Stylianopoulos T: The role of mechanical forces in tumor growth and therapy. *Annu Rev Biomed Eng* 16: 321-346, 2014.
- Senger DR, Galli SJ, Dvorak AM, Perruzzi CA, Harvey VS and Dvorak HF: Tumor cells secrete a vascular permeability factor that promotes accumulation of ascites fluid. *Science* 219: 983-985, 1983.
- Liu YL, Horning AM, Lieberman B, Kim M, Lin CK, Hung CN, Chou CW, Wang CM, Lin CL, Kirma NB, *et al*: Spatial EGFR dynamics and metastatic phenotypes modulated by upregulated EphB2 and Src pathways in advanced prostate cancer. *Cancers (Basel)* 11: 1910, 2019.
- Sato S, Vasaiak S, Eskaros A, Kim Y, Lewis JS, Zhang B, Zijlstra A and Weaver AM: EPHB2 carried on small extracellular vesicles induces tumor angiogenesis via activation of ephrin reverse signaling. *JCI Insight* 4: e132447, 2019.
- Makaryan V, Zeidler C, Bolyard AA, Skokowa J, Rodger E, Kelley ML, Boxer LA, Bonilla MA, Newburger PE, Shimamura A, *et al*: The diversity of mutations and clinical outcomes for ELANE-associated neutropenia. *Curr Opin Hematol* 22: 3-11, 2015.
- Nakashima R, Goto Y, Koyasu S, Kobayashi M, Morinibu A, Yoshimura M, Hiraoka M, Hammond EM and Harada H: UCHL1-HIF-1 axis-mediated antioxidant property of cancer cells as a therapeutic target for radiosensitization. *Sci Rep* 7: 6879, 2017.
- Semenza GL: Pharmacologic targeting of hypoxia-inducible factors. *Annu Rev Pharmacol Toxicol* 59: 379-403, 2019.
- Zhong H, De Marzo AM, Laughner E, Lim M, Hilton DA, Zagzag D, Buechler P, Isaacs WB, Semenza GL and Simons JW: Overexpression of hypoxia-inducible factor 1 α in common human cancers and their metastases. *Cancer Res* 59: 5830-5835, 1999.
- Talks KL, Turley H, Gatter KC, Maxwell PH, Pugh CW, Ratcliffe PJ and Harris AL: The expression and distribution of the hypoxia-inducible factors HIF-1 α and HIF-2 α in normal human tissues, cancers, and tumor-associated macrophages. *Am J Pathol* 157: 411-421, 2000.
- Generali D, Berruti A, Brizzi MP, Campo L, Bonardi S, Wigfield S, Bersiga A, Allevi G, Milani M, Aguggini S, *et al*: Hypoxia-inducible factor-1 α expression predicts a poor response to primary chemoendocrine therapy and disease-free survival in primary human breast cancer. *Clin Cancer Res* 12: 4562-4568, 2006.
- Aebersold DM, Burri P, Beer KT, Laissue J, Djonov V, Greiner RH and Semenza GL: Expression of hypoxia-inducible factor-1 α : A novel predictive and prognostic parameter in the radiotherapy of oropharyngeal cancer. *Cancer Res* 61: 2911-2916, 2001.
- Nanni S, Benvenuti V, Grasselli A, Priolo C, Aiello A, Mattiussi S, Colussi C, Lirangi V, Illi B, D'Eletto M, *et al*: Endothelial NOS, estrogen receptor beta, and HIFs cooperate in the activation of a prognostic transcriptional pattern in aggressive human prostate cancer. *J Clin Invest* 119: 1093-1108, 2009.

32. Semenza GL: Defining the role of hypoxia-inducible factor 1 in cancer biology and therapeutics. *Oncogene* 29: 625-634, 2010.
33. Apte RS, Chen DS and Ferrara N: VEGF in signaling and disease: Beyond discovery and development. *Cell* 176: 1248-1264, 2019.
34. Dvorak HF: Vascular permeability factor/vascular endothelial growth factor: A critical cytokine in tumor angiogenesis and a potential target for diagnosis and therapy. *J Clin Oncol* 20: 4368-4380, 2002.
35. Kellar A, Egan C and Morris D: Preclinical murine models for lung cancer: Clinical trial applications. *Biomed Res Int* 2015: 621324, 2015.
36. Mori T, Koga T, Shibata H, Ikeda K, Shiraishi K, Suzuki M and Iyama K: Interstitial fluid pressure correlates clinicopathological factors of lung cancer. *Ann Thorac Cardiovasc Surg* 21: 201-208, 2015.

Nicaraven mitigates radiation-induced lung injury by downregulating the NF- κ B and TGF- β /Smad pathways to suppress the inflammatory response

Yong Xu^{1,2}, Da Zhai^{1,2}, Shinji Goto^{1,2}, Xu Zhang^{1,2}, Keiichi Jingu³ and Tao-Sheng Li^{1,2,*}

¹Department of Stem Cell Biology, Atomic Bomb Disease Institute, Nagasaki University, Nagasaki 852-8523, Japan

²Department of Stem Cell Biology, Nagasaki University Graduate School of Biomedical Sciences, 1-12-4 Sakamoto, Nagasaki 852-8523, Japan

³Department of Radiation Oncology, Graduate School of Medicine, Tohoku University, Sendai 980-8574, Japan.

*Corresponding author: Department of Stem Cell Biology, Atomic Bomb Disease Institute, Nagasaki University, 1-12-4 Sakamoto, Nagasaki 852-8523, Japan. Tel: +81-95-819-7099; Fax: +81-95-819-7100, E-mail: litaoshe@nagasaki-u.ac.jp

(Received 23 June 2021; revised 16 August 2021; editorial decision 29 October 2021)

ABSTRACT

Radiation-induced lung injury (RILI) is commonly observed in patients receiving radiotherapy, and clinical prevention and treatment remain difficult. We investigated the effect and mechanism of nicaraven for mitigating RILI. C57BL/6 N mice (12-week-old) were treated daily with 6 Gy X-ray thoracic radiation for 5 days in sequences (cumulative dose of 30 Gy), and nicaraven (50 mg/kg) or placebo was injected intraperitoneally in 10 min after each radiation exposure. Mice were sacrificed and lung tissues were collected for experimental assessments at the next day (acute phase) or 100 days (chronic phase) after the last radiation exposure. Of the acute phase, immunohistochemical analysis of lung tissues showed that radiation significantly induced DNA damage of the lung cells, increased the number of Sca-1⁺ stem cells, and induced the recruitment of CD11c⁺, F4/80⁺ and CD206⁺ inflammatory cells. However, all these changes in the irradiated lungs were effectively mitigated by nicaraven administration. Western blot analysis showed that nicaraven administration effectively attenuated the radiation-induced upregulation of NF- κ B, TGF- β , and pSmad2 in lungs. Of the chronic phase, nicaraven administration effectively attenuated the radiation-induced enhancement of α -SMA expression and collagen deposition in lungs. In conclusion we find that nicaraven can effectively mitigate RILI by downregulating NF- κ B and TGF- β /pSmad2 pathways to suppress the inflammatory response in the irradiated lungs.

Keywords: radiation; DNA damage; lung injury; inflammatory response

INTRODUCTION

Radiotherapy is used for cancer treatment, but exposure to high doses of ionizing radiation also damages the normal tissue cells [1, 2]. Radiation-induced lung injury (RILI), including acute pneumonitis and chronic pulmonary fibrosis, is frequently observed in patients receiving thoracic radiotherapy. It is estimated that RILI occurs in 13–37% of lung cancer patients undergoing curative radiotherapy, which may limit the dose of radiotherapy and affect the quality of life [3]. Currently, the pathogenesis of RILI has not yet been fully understood, and there is no effective drug in the clinic.

It is known that high dose ionizing radiation leads to DNA double-strand breaks [4]. DNA damage contributes to oxidative stress, vascular damage, and inflammation. Pneumonitis develops within hours

or days after high dose irradiation exposure, and is accompanied by an increased capillary permeability and the accumulation of inflammatory cells in lungs [5–7]. The recruited inflammatory cells secrete profibrotic cytokines to activate the resident fibroblasts, which finally leads to an excessive collagen production and deposition in the interstitial space of lungs [8–10].

NF- κ B (nuclear factor kappa B) is an important regulator of inflammatory response. The NF- κ B signaling pathway is known to be activated following radiation exposure [11]. TGF- β /Smad signaling pathway also deeply involves in RILI [12, 13]. Thoracic irradiation causes a continuous increase of TGF- β ₁ in plasma, which is a predictor of radiation pneumonitis after radiotherapy [14]. The activation of TGF- β induces the conversion of fibroblasts into myofibroblasts, the elevated

expression of α -smooth muscle actin (α -SMA), and the synthesis of extracellular matrix proteins such as collagen [15, 16]. Therefore, targeting these pathways can be a potential strategy for mitigating RILI.

Nicaraven, a hydroxyl free radical scavenger [17], has previously been demonstrated to protect against the radiation-induced cell death [18, 19]. We have also recently found that the administration of nicaraven to mice soon after high dose γ -ray exposure attenuates the radiation-induced injury of hematopoietic stem/progenitor cells, which is more likely associated with anti-inflammatory effect rather than radical scavenging [20, 21]. Moreover, nicaraven can reduce the radiation-induced recruitment of macrophages and neutrophils into lungs [22]. Therefore, we speculate that nicaraven may effectively mitigate RILI, at least partly by inhibiting inflammatory response through NF- κ B and TGF- β /Smad signaling pathways [23].

By exposing the lungs of adult mice to 30 Gy X-ray, we investigated the effect and mechanism of nicaraven for mitigating RILI. Our results showed that nicaraven administration significantly reduced the DNA damage of lung tissue (stem) cells, inhibited the radiation-induced recruitment of CD11c⁺, F4/80⁺ and CD206⁺ inflammatory cells in lungs at the acute phase, and also mitigated the radiation-induced enhancement of α -SMA and partly decreased the fibrotic area in the irradiated lungs at the chronic phase.

MATERIALS AND METHODS

Animals

Male C57BL/6 N mice (12-week-old; CLEA, Japan) were used for study. Mice were housed in pathogen-free room with a controlled environment under a 12 h light–dark cycle, with free access to food and water. This study was approved by the Institutional Animal Care and Use Committee of Nagasaki University (No.1608251335-12). All animal procedures were performed in accordance with institutional and national guidelines.

Thoracic radiation exposure and nicaraven administration

The RILI model was established as previously described [24]. Briefly, mice were treated daily with 6 Gy X-ray thoracic radiation for 5 days in sequences (cumulative dose of 30 Gy) at a dose rate of 1.0084 Gy/min (200 kV, 15 mA, 5 mm Al filtration, ISOVOLT TITAN320, General Electric Company, United States) (Supplementary Fig. 1A). Nicaraven (50 mg/kg; n = 6, IR + N group) or placebo (n = 6, IR group) was injected intraperitoneally to mice within 10 min after each radiation exposure, and we continued the daily injections for 5 additional days after the last radiation exposure (Supplementary Fig. 1A). Age-matched mice without radiation exposure were used as control (n = 6, CON group). The body weights of mice were recorded once a week. We sacrificed the mice the next day (Acute phase) or the 100th day (Chronic phase) after the last exposure (Supplementary Fig. 1A). At the end of follow-up, mice were euthanized under general anesthesia by severing the aorta to remove the blood. Lung tissues were excised and weighed, and then collected for experimental evaluations as follows.

Immunohistochemical analysis

The DNA damage in lung tissue (stem) cells was detected by immunohistochemical analysis. Briefly, lungs were fixed in 4% paraformaldehyde, and paraffin sections of 6- μ m-thick were deparaffinized and rehydrated. After antigen retrieval and blocking, sections were incubated with rabbit anti-mouse γ -H2AX antibody (1:400 dilution, Abcam) and rat anti-mouse Sca-1 antibody (1:200 dilution, Abcam) overnight at 4°C, and followed by the appropriate fluorescent-conjugated secondary antibodies at 25°C for 60 min. The nuclei were stained with 4, 6-diamidino-2-phenylindole (DAPI) (1:1000 dilution, Life technologies). The positive staining was examined under fluorescence microscope (FV10CW3, OLYMPUS).

The recruitment of inflammatory cells was detected by immunostaining with mouse anti-mouse CD11c antibody (1:150 dilution, Abcam), rat anti-mouse F4/80 antibody (1:100 dilution, Abcam), goat anti-mouse CD206 antibody (1:200 dilution, R&D Systems) overnight at 4°C, and followed by the appropriate Alexa fluorescent-conjugated secondary antibodies (1:400 dilution, Invitrogen), respectively. The nuclei were stained with DAPI. The positive staining was examined under fluorescence microscope (FV10CW3, OLYMPUS).

For quantitative analysis, we counted the positively stained cells in 12 images from two separated independent sections of each lung tissue sample. The number of positively stained cells in each lung tissue sample was normalized by the number of nuclei, and the average value per field (image) from each lung tissue sample was used for statistical analysis.

Masson's trichrome staining

To detect the fibrotic change in lungs, Masson's trichrome staining was performed according to the manufacturer's protocol (Sigma-Aldrich, St. Louis, MO, USA). The stained sections were mounted and then imaged using a microscope (Biorevo BZ-9000; Keyence Japan, Osaka, Japan). The fibrotic area was quantified by measuring the positively stained area using the Image-Pro Plus software (version 5.1.2, Media Cybernetics Inc, Carlsbad, CA, USA), and expressed as a percentage of the total area. The average value from 12 images randomly selected from two separated slides for each lung tissue sample was used for statistical analysis.

Western blot

Western blot was performed as previously described [25]. Briefly, lung tissue sample was homogenized using Multi-beads shocker[®] and added to the T-PER reagent (Thermo Fisher Scientific) consisting of proteinase and dephosphorylation inhibitors (Thermo Fisher Scientific). Total tissue protein purified from lungs were separated by SDS-PAGE gels and then transferred to 0.22- μ m PVDF membranes (Bio-Rad). After blocking, the membranes were incubated with primary antibodies against NF- κ B p65 (1:500 dilution, Abcam), I κ B α (1:1000 dilution, CST), TGF- β (1:1000 dilution, Abcam), pSmad2 (1:1000 dilution, Abcam), α -Tubulin (1:1000 dilution, CST), or GAPDH (1:1000 dilution, Abcam), respectively; and followed by the appropriate horseradish peroxidase-conjugated secondary antibodies (Dako). The expression was visualized using an enhanced chemiluminescence detection kit (Thermo Scientific).

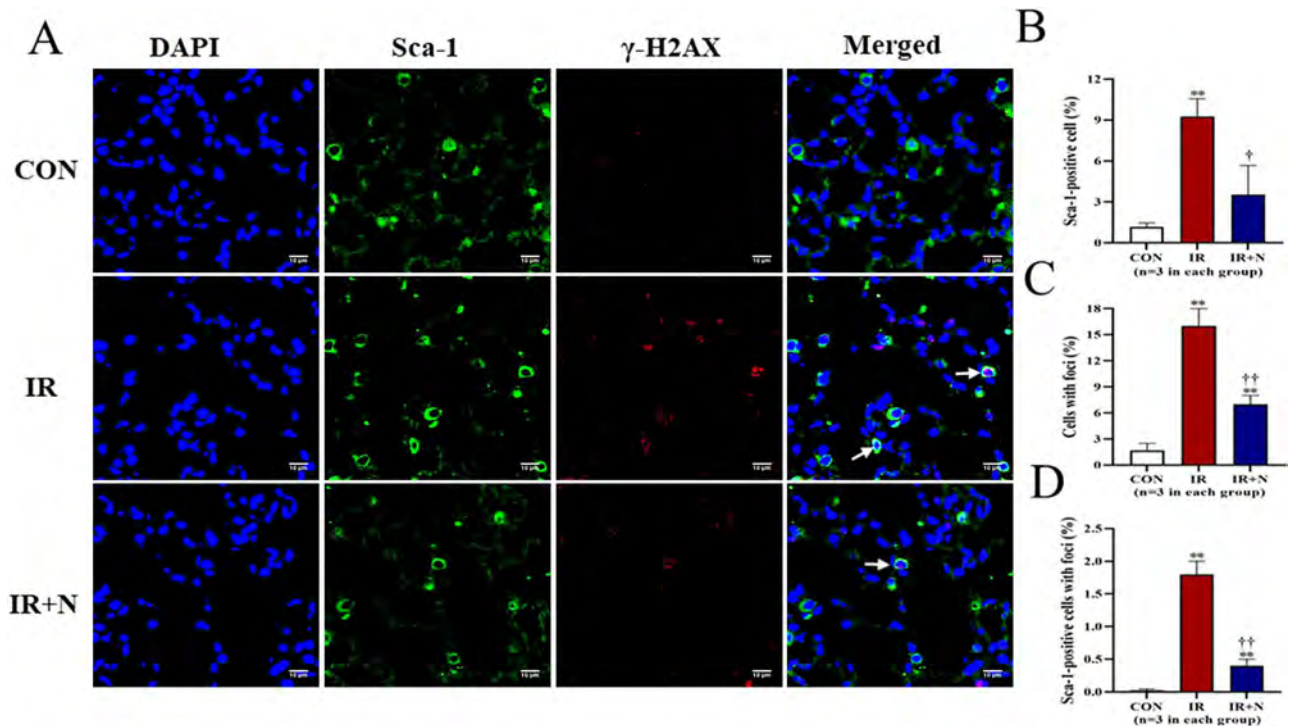


Fig. 1. The DNA damage of lung tissue cells at the acute phase after treatments. (A) Representative confocal images show the expression of Sca-1 and γ -H2AX in lung tissue cells. Quantitative data on the number of Sca-1⁺ stem cells (B), the total cells with γ -H2AX foci formation (C), and the Sca-1⁺ stem cells with γ -H2AX foci formation (D, Arrows) are shown. Scale bars: 10 μ m. The nuclei were stained with DAPI. Data are represented as means \pm SD. ** $p < 0.01$ vs CON group, † $p < 0.05$, †† $p < 0.01$ vs IR group. CON: Control, IR: Radiation, IR + N: Radiation+Nicaraven.

Semiquantitative analysis was done using ImageQuant LAS 4000 mini (GE Healthcare Life Sciences).

Statistical analysis

All the values were presented as mean \pm SD. For comparison of multiple sets of data, one-way analysis of variance (ANOVA) followed by Tukey's test (Dr. SPSS II, Chicago, IL) was used. For comparison of two sets of data, an unpaired two-tailed t -test was used. All analysis was carried out with the SPSS19.0 statistical software (IBM SPSS Co., USA). A p -value less than 0.05 was accepted as significant.

RESULTS

Nicaraven significantly reduced the radiation-induced DNA damage of lung tissue (stem) cells at the acute phase.

All mice survived after treatments and during the follow-up period. The body weights of the mice were decreased temporarily soon after radiation exposure, but tended to increase approximately 10 days after radiation exposure. Although the body weights of mice between IR group and IR + N group were not significantly different, they were significantly lower than the age-matched non-irradiated mice in the CON group ($p < 0.05$, Supplementary Fig. 1B). Moreover, the lung weights of mice were not significantly different among all groups at either the acute phase or the chronic phase (Supplementary Fig. 1C).

Immunohistochemistry was performed to evaluate the expression of Sca-1 and γ -H2AX in lung tissue cells at the acute phase (Fig. 1A). Compared to CON group, the number of Sca-1⁺ stem cells was significantly increased in the IR group ($9.27 \pm 1.30\%$ vs $1.17 \pm 0.29\%$, $p < 0.01$; Fig. 1B). However, the increased number of Sca-1⁺ stem cells in irradiated lungs was significantly attenuated by nicaraven administration ($3.53 \pm 2.15\%$, $p < 0.05$ vs IR group; Fig. 1B).

The formation of γ -H2AX foci in nuclei of lung tissue cells was dramatically increased in the IR group, but was mildly changed in the IR + N group (Fig. 1A). Quantitative data also indicated that the percentage of γ -H2AX-positive cells was significantly less in the IR + N group than the IR group ($7.13 \pm 0.91\%$, $p < 0.01$; Fig. 1C). Moreover, we tried to evaluate the formation of γ -H2AX foci in Sca-1⁺ stem cells. Interestingly, the number of Sca-1⁺ stem cells with γ -H2AX foci was more effectively decreased in the IR + N group compared to the IR group ($1.93 \pm 0.51\%$ vs $0.35 \pm 0.19\%$, $p < 0.01$; Fig. 1D). These results indicate that nicaraven administration can reduce the radiation-induced DNA damage in lung tissue cells, especially in these Sca-1⁺ stem cells.

Nicaraven effectively decreased the radiation-induced recruitment of inflammatory cells into lungs.

According to our previous studies [20, 21], nicaraven protects tissue (stem) cells against radiation injury by inhibiting

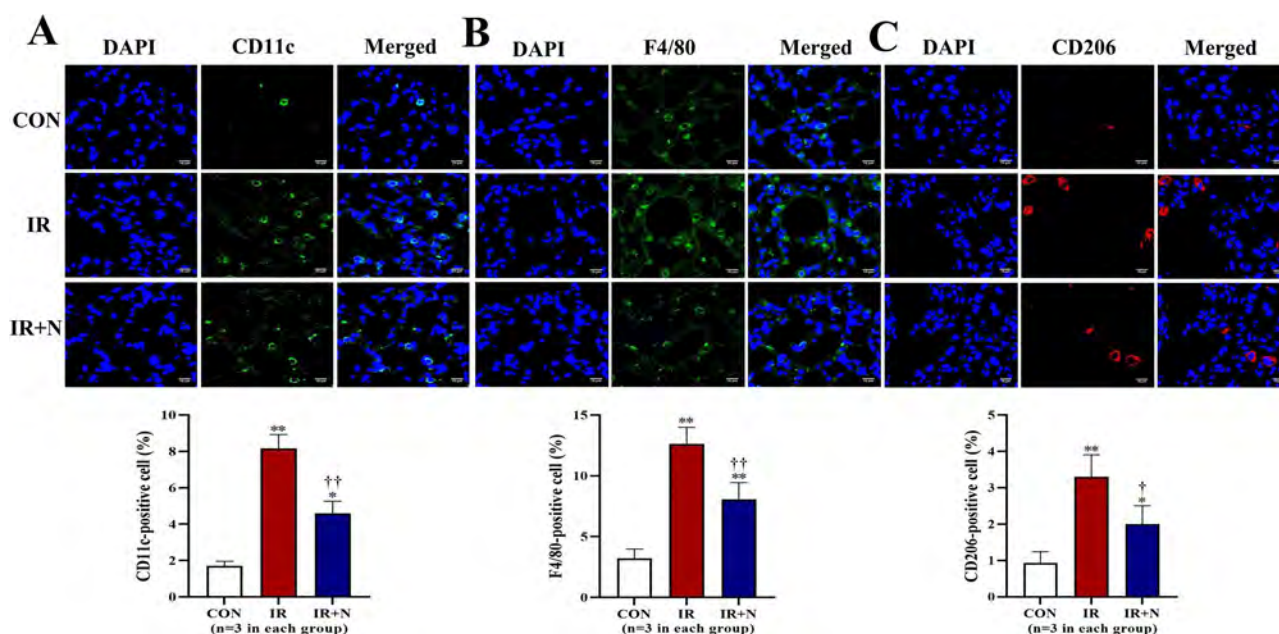


Fig. 2. Immunohistochemical detection of inflammatory cells in lungs at the acute phase after treatments. Representative confocal images (upper) and quantitative data (lower) show the CD11c⁺ cells (A), F4/80⁺ cells (B), and CD206⁺ cells (C) in lungs. Scale bars: 10 μ m. The nuclei were stained with DAPI. Data are represented as means \pm SD. * p < 0.05, ** p < 0.01 vs CON group, † p < 0.05, †† p < 0.01 vs IR group. CON: Control, IR: Radiation, IR + N: Radiation+Nicaraven.

inflammatory response. Therefore, immunohistochemical analysis was performed to detect the inflammatory cells in lungs. The number of CD11c⁺ monocytes and F4/80⁺ macrophages was significantly higher in the IR group than the CON group (p < 0.01, Fig. 2A and B). However, nicaraven administration significantly reduced the recruitment of CD11c⁺ monocytes ($8.23 \pm 0.75\%$ vs $4.61 \pm 0.65\%$, p < 0.01; Fig. 2A) and F4/80⁺ macrophages ($12.63 \pm 1.36\%$ vs $8.07 \pm 1.38\%$, p < 0.01; Fig. 2B) into irradiated lungs. Similarly, the number of M2 macrophages (CD206⁺) was also significantly higher in irradiated lungs than that of non-irradiated lungs (p < 0.01, Fig. 2C). Interestingly, nicaraven administration significantly decreased the CD206⁺ macrophages in irradiated lungs ($3.3 \pm 0.61\%$ vs $2.1 \pm 0.53\%$, p < 0.05; Fig. 2C).

Nicaraven significantly attenuated the radiation-induced upregulation of NF- κ B and TGF- β in lungs

To further understand the molecular mechanism of nicaraven on mitigating RILI, we investigated the expression of NF- κ B and I κ B α (inhibitor of NF- κ B) in lungs at the acute phase. Compared to the CON group, the IR group showed a significant enhancement on the expression of NF- κ B (p < 0.05, Fig. 3A). However, the enhanced expression of NF- κ B in irradiated lungs was effectively attenuated by nicaraven administration ($p = 0.09$, Fig. 3A). In contrast, the expression of total I κ B α was significantly decreased in irradiated lungs (p < 0.01 vs CON group, Fig. 3B), which was effectively attenuated by nicaraven administration (p < 0.01 vs IR group, Fig. 3B). We also investigated the expression of TGF- β and pSmad2 in irradiated lungs at the acute phase (Fig. 3C and D). The irradiated lungs showed a

significant upregulation of TGF- β and pSmad2 (p < 0.05 vs CON group, Fig. 3C and D), but was effectively attenuated by nicaraven administration (p < 0.05 vs IR group, Fig. 3C and D).

Nicaraven clearly attenuated the radiation-induced enhancement of α -SMA and partially reduced the fibrotic area in irradiated lungs at the chronic phase

We further investigated the expression of α -SMA and collagen deposition in irradiated lungs at the chronic phase. Western blot indicated an enhanced expression of α -SMA in the irradiated lungs (p < 0.05 vs CON group, Fig. 4A), but the enhanced expression of α -SMA in irradiated lungs was completely attenuated by nicaraven administration (Fig. 4A). Similarly, Masson's trichrome staining showed that the fibrotic area in lungs was significantly higher in the IR group than the CON group (p < 0.05, Fig. 4B). However, nicaraven administration tended to only partially reduce the fibrotic area in irradiated lungs ($6.24 \pm 0.64\%$ vs $5.14 \pm 0.51\%$, $p = 0.08$; Fig. 4B).

DISCUSSION

This study was proposed to investigate the potential effect and underlying mechanism of nicaraven on mitigating RILI. Our experimental data revealed that nicaraven administration not only reduced the DNA damage (γ -H2AX foci formation) of lung tissue (stem) cells, but also inhibited the recruitment of macrophages and neutrophils into irradiated lungs at the acute phase. Nicaraven administration also significantly attenuated the radiation-induced enhancement of TGF- β and NF- κ B, and partially reduced the fibrotic area in irradiated lungs at the chronic phase.

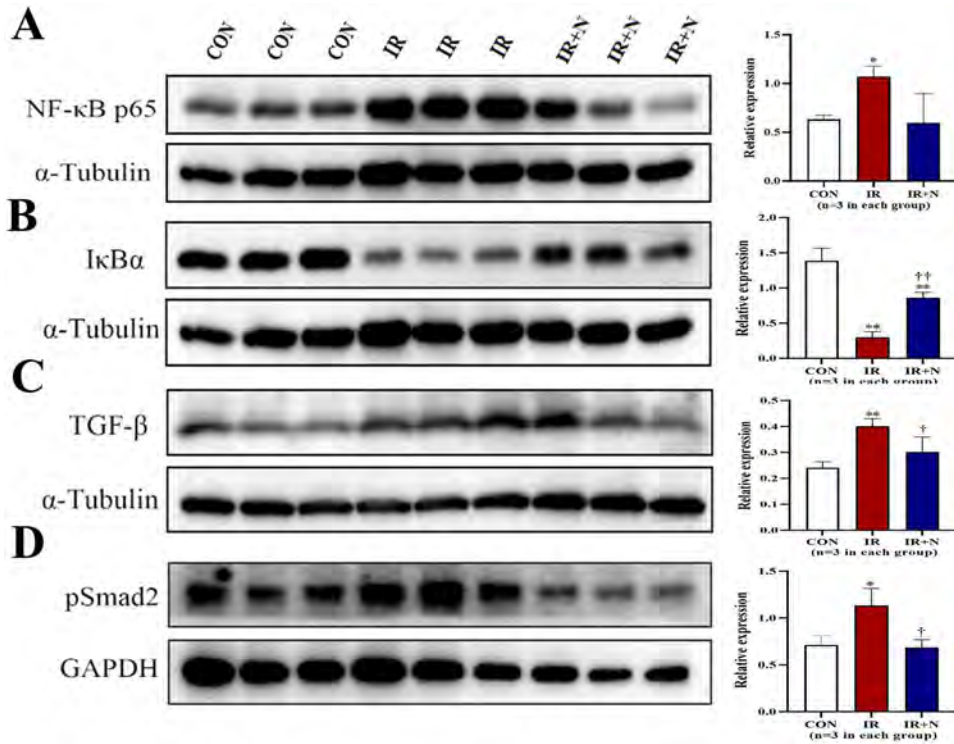


Fig. 3. Western blot analysis on the expression of NF-κB, IκBα, TGF-β, and pSmad2 in lungs. Representative blots (left) and quantitative data (right) on the expression of NF-κB p65 (A), IκBα (B), TGF-β (C), pSmad2 (D) in lungs are shown. Data are normalized to α-Tubulin or GAPDH, and represented as means ± SD. *p < 0.05, **p < 0.01 vs CON group, †p < 0.05, ††p < 0.01 vs IR group. CON: Control, IR: Radiation, IR + N: Radiation+Nicaraven.

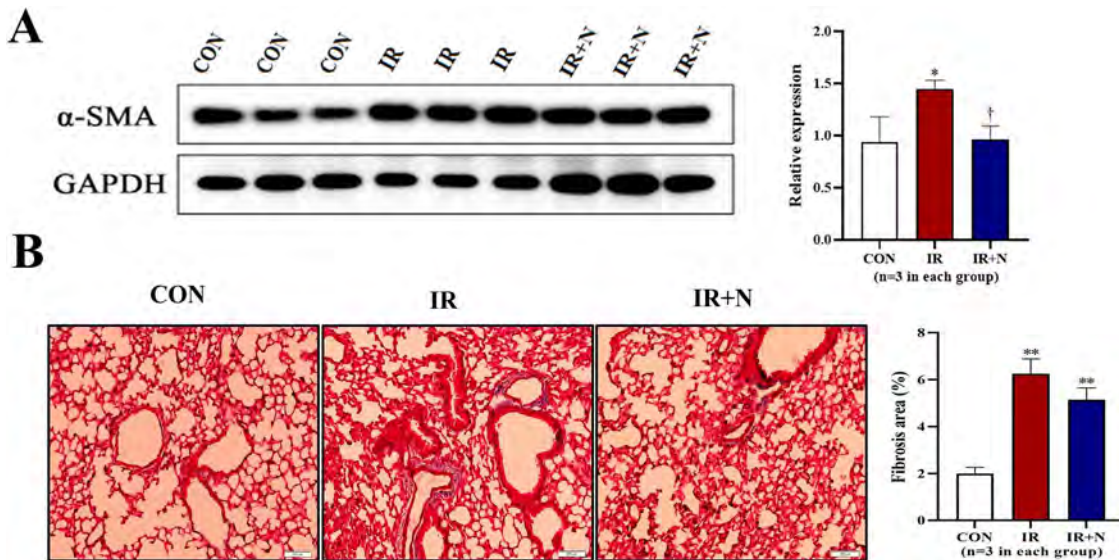


Fig. 4. The fibrotic changes in lungs at the chronic phase after treatments. (A) Representative blots (left) and quantitative data (right) on the expression of α-SMA in lungs are shown. (B) Representative images (left) and quantitative data (right) of Masson's trichrome staining on the fibrotic area in lungs are shown. Scale bars: 200 μm. Data are represented as means ± SD. *p < 0.05, **p < 0.01 vs CON group, †p < 0.05 vs IR group. CON: Control, IR: Radiation, IR + N: Radiation+Nicaraven.

Nicaraven is known as a powerful radical scavenger that effectively protects various tissues and organs against injuries, particularly for ischemia–reperfusion injury in the brain [26–28]. Considering the well-recognized antioxidative property and the potential anti-inflammatory effect of nicaraven, we evaluated the probable role of nicaraven on mitigating RILI.

The exposure to high levels of ionizing radiation leads to DNA double-strand breaks, which elicit cell death or stochastic change [4]. Stem cells are known to play critical role in tissue homeostasis, while ionizing radiation exposure can disrupt the tissue homeostasis. Alveolar epithelium is composed of two cell types: Type I cells account for 95% of the gas exchange surface area, and type II cells can transform into type I cells and have the ability to repair alveoli. Sca-1-positive cells are identified as a population of alveolar type II cells with progenitor cell properties [29]. It has also been demonstrated that the proliferation of Sca-1-positive cells increases during the alveolar epithelial repair phase [29, 30]. In this study, the number of Sca-1-positive cells were exactly increased in irradiated lungs at the acute phase, suggesting the probable role of Sca-1-positive cells for repairing the injured lungs after high dose irradiation. Nicaraven administration showed to reduce the DNA damage of lung tissue cells, especially in these Sca-1-positive cells at the acute phase, which indirectly indicates the protective effect of nicaraven on RILI.

Various chemokines/cytokines are known to be increased in organs/tissues exposed to high dose irradiation, which in turn induces the recruitment of inflammatory cells at the acute phase. The recruited inflammatory cells play a key role in the pathogenesis of RILI [31, 32], because inflammatory cascade is known to promote fibroblast proliferation and collagen deposition [33]. In responding to high dose radiation exposure, the recruitment of monocytes/immune cells (CD11c⁺) into lung tissue plays critical pathophysiological role on RILI. Among the recruited monocytes/immune cells, macrophages (F4/80⁺) represent an important profibrogenic initiator/mediator, but M2 macrophages (CD206⁺) are thought to be an anti-inflammatory phenotype of macrophages. In this study, we found that the recruitment of monocytes/immune cells, including the M2 macrophages was significantly increased in the irradiated lungs. Consistent with previous reports [22, 34], the administration of nicaraven inhibited significantly the recruitment of monocytes into the irradiated lungs. It will be better to understand the precise role of especial subpopulation of inflammatory cells, such as the M2 macrophages in lungs using genetically modified animals. However, the purpose of this study was designed to examine the potency of nicaraven for attenuating RILI through an anti-inflammatory mechanism, we used a wild-type mice rather than the genetically modified mice for experiments.

TGF- β is one of the most critical master regulators on promoting acute inflammation and chronic fibrosis in lungs [12–16]. Previous studies have demonstrated that radiation exposure activates TGF- β /Smad signaling pathway to initiate the inflammatory response, induce the proliferation and activation of fibroblasts, and enhance the synthesis of matrix proteins [35, 36]. Therefore, the inhibition of TGF- β /Smad signaling pathway may effectively mitigate RILI. In this study, nicaraven administration exactly downregulated the expression of TGF- β and pSmad2 in irradiated lungs at the acute phase.

NF- κ B has emerged as a ubiquitous factor involved in the regulation of numerous critical processes, including immune [37], inflammation response [38], cell apoptosis [39], and cell proliferation [40]. While in an inactivated state, NF- κ B is located in the cytosol complexed with the inhibitory protein I κ B α . Radiation exposure can activate NF- κ B signaling pathway. Radiation exposure activates the kinase IKK, which in turn phosphorylates I κ B α and results in ubiquitin-dependent degradation [11, 38, 40]. Dysregulation of NF- κ B signaling can lead to inflammation, autoimmune disease and cancer [41]. In this study, nicaraven administration effectively downregulated the expression of NF- κ B, suggesting the involvement of NF- κ B pathway in the protective effect of nicaraven to RILI.

Generally, although nicaraven administration only tended to partially reduce the fibrotic area in the irradiated lungs, many other parameters, such as the expression of α -SMA was more sensitively and clearly changed. As the activated fibroblasts (α -SMA⁺) are generally thought to be the predominant source of collagen-producing cells, the inhibition on α -SMA expression in irradiated lungs by nicaraven administration suggested the probable benefit of nicaraven for attenuating the development of fibrotic change in irradiated lungs at the chronic phase. In summary, nicaraven administration effectively protected the RILI, likely by suppressing inflammatory response through the NF- κ B and TGF- β /Smad signaling pathways. Nicaraven could be a potential drug for mitigating RILI.

SUPPLEMENTARY DATA

Supplementary data is available at *RADRES Journal* online.

ACKNOWLEDGEMENTS

This study was supported by the Agency for Medical Research and Development under Grant Number JP20lm0203081. The funder played no role in study design, data collection and analysis, decision to publish, or manuscript preparation.

CONFLICT OF INTEREST

The authors indicate no potential conflicts of interest.




REFERENCES

1. Bentzen SM. Preventing or reducing late side effects of radiation therapy: radiobiology meets molecular pathology. *Nat Rev Cancer* 2006;6:702–13.
2. McBride WH, Schae D. Radiation-induced tissue damage and response. *J Pathol* 2020;250:647–55.
3. Rodrigues G, Lock M, D'Souza D et al. Prediction of radiation pneumonitis by dose volume histogram parameters in lung cancer—a systematic review. *Radiother Oncol* 2004;71:127–38.
4. Huang L, Snyder AR, Morgan WF. Radiation-induced genomic instability and its implications for radiation carcinogenesis. *Oncogene* 2003;22:5848–54.
5. Hanania AN, Mainwaring W, Ghebre YT et al. Radiation-induced lung injury: assessment and management. *Chest* 2019;156:150–62.

6. Giuranno L, Ient J, De Ruyscher D et al. Radiation-induced lung injury (RILI). *Front Oncol* 2019;9:877.
7. Kim H, Park SH, Han SY et al. LXA4-FPR2 signaling regulates radiation-induced pulmonary fibrosis via crosstalk with TGF- β /Smad signaling. *Cell Death Dis* 2020;11:653.
8. Jin H, Yoo Y, Kim Y et al. Radiation-induced lung fibrosis: pre-clinical animal models and therapeutic strategies. *Cancers (Basel)* 2020;12:1561.
9. Kainthola A, Haritwal T, Tiwari M et al. Immunological aspect of radiation-induced pneumonitis, current treatment strategies, and future prospects. *Front Immunol* 2017;8:506.
10. Im J, Lawrence J, Seelig D et al. FoxM1-dependent RAD51 and BRCA2 signaling protects idiopathic pulmonary fibrosis fibroblasts from radiation-induced cell death. *Cell Death Dis* 2018;9:584.
11. Devary Y, Rosette C, DiDonato JA et al. NF-kappa B activation by ultraviolet light not dependent on a nuclear signal. *Science* 1993;261:1442–5.
12. Madani I, De Ruyck K, Goeminne H et al. Predicting risk of radiation-induced lung injury. *J Thorac Oncol* 2007;2:864–74.
13. Fleckenstein K, Gauter-Fleckenstein B, Jackson IL et al. Using biological markers to predict risk of radiation injury. *Semin Radiat Oncol* 2007;17:89–98.
14. Anscher MS, Kong FM, Andrews K et al. Plasma transforming growth factor beta1 as a predictor of radiation pneumonitis. *Int J Radiat Oncol Biol Phys* 1998;41:1029–35.
15. Singh V, Torricelli AA, Nayeb-Hashemi N et al. Mouse strain variation in SMA(+) myofibroblast development after corneal injury. *Exp Eye Res* 2013;115:27–30.
16. Tatler AL, Jenkins G. TGF- β activation and lung fibrosis. *Proc Am Thorac Soc* 2012;9:130–6.
17. Akimoto T. Quantitative analysis of the kinetic constant of the reaction of N,N'-propylenedini-cotinamide with the hydroxyl radical using dimethyl sulfoxide and deduction of its structure in chloroform. *Chem Pharm Bull(Tokyo)* 2000;48:467–76.
18. Mori Y, Takashima H, Seo H et al. Experimental studies on Nicaraven as radioprotector-free radical scavenging effect and the inhibition of the cellular injury. *Nihon Igaku Hoshasen Gakkai Zasshi* 1993;53:704–12.
19. Watanabe M, Akiyama N, Sekine H et al. Inhibition of poly (ADP-ribose) polymerase as a protective effect of nicaraven in ionizing radiation- and ara-C-induced cell death. *Anticancer Res* 2006;26:3421–7.
20. Zingarelli B, Scott GS, Hake P et al. Effects of nicaraven on nitric oxide-related pathways and in shock and inflammation. *Shock* 2000;13:126–34.
21. Masana Y, Yoshimine T, Fujita T et al. Reaction of microglial cells and macrophages after cortical incision in rats: effect of a synthesized free radical scavenger, (+/-)-N,N'-propylenediniticotinamide (AVS). *Neurosci Res* 1995;23:217–21.
22. Yan C, Luo L, Urata Y et al. Nicaraven reduces cancer metastasis to irradiated lungs by decreasing CCL8 and macrophage recruitment. *Cancer Lett* 2018;418:204–10.
23. Lin H, Wu X, Yang Y et al. Nicaraven inhibits TNF α -induced endothelial activation and inflammation through suppressing NF- κ B signaling pathway. *Can J Physiol Pharmacol* 2021;99:803–11.
24. Citrin DE, Shankavaram U, Horton JA et al. Role of type II pneumocyte senescence in radiation-induced lung fibrosis. *J Natl Cancer Inst* 2013;105:1474–84.
25. Doi H, Kitajima Y, Luo L et al. Potency of umbilical cord blood- and Wharton's jelly-derived mesenchymal stem cells for scarless wound healing. *Sci Rep* 2016;6:18844.
26. Asano T, Johshita H, Koide T et al. Amelioration of ischaemic cerebral oedema by a free radical scavenger, AVS: 1,2-bis(nicotinamido)-propane. An experimental study using a regional ischaemia model in cats. *Neurol Res* 1984;6:163–8.
27. Asano T, Takakura K, Sano K et al. Effects of a hydroxyl radical scavenger on delayed ischemic neurological deficits following aneurysmal subarachnoid hemorrhage: results of a multicenter, placebo-controlled double-blind trial. *J Neurosurg* 1996;84:792–803.
28. Imperatore C, Germanò A, d'Avella D et al. Effects of the radical scavenger AVS on behavioral and BBB changes after experimental subarachnoid hemorrhage. *Life Sci* 2000;66:779–90.
29. Liu Y, Kumar VS, Zhang W et al. Activation of type II cells into regenerative stem cell antigen-1(+) cells during alveolar repair. *Am J Respir Cell Mol Biol* 2015;53:113–24.
30. Liu Y, Sadikot RT, Adami GR et al. FoxM1 mediates the progenitor function of type II epithelial cells in repairing alveolar injury induced by *Pseudomonas aeruginosa*. *J Exp Med* 2011;208:1473–84.
31. Johnston CJ, Williams JP, Elder A et al. Inflammatory cell recruitment following thoracic irradiation. *Exp Lung Res* 2004;30:369–82.
32. Meziani L, Deutsch E, Mondini M. Macrophages in radiation injury: a new therapeutic target. *Onco Targets Ther* 2018;7:e1494488.
33. Boothe DL, Coplowitz S, Greenwood E et al. Transforming growth factor β -1 (TGF- β 1) is a serum biomarker of radiation induced fibrosis in patients treated with intracavitary accelerated partial breast irradiation: preliminary results of a prospective study. *Int J Radiat Oncol Biol Phys* 2013;87:1030–6.
34. Zhang X, Moriwaki T, Kawabata T et al. Nicaraven attenuates postoperative systemic inflammatory responses-induced tumor metastasis. *Ann Surg Oncol* 2020;27:1068–74.
35. Meng XM, Nikolic-Paterson DJ, Lan HY. TGF- β : the master regulator of fibrosis. *Nat Rev Nephrol* 2016;12:325–38.
36. Samarakoon R, Overstreet JM, Higgins PJ. TGF- β signaling in tissue fibrosis: redox controls, target genes and therapeutic opportunities. *Cell Signal* 2013;25:264–8.
37. Baeuerle PA, Henkel T. Function and activation of NF-kappa B in the immune system. *Annu Rev Immunol* 1994;12:141–79.
38. Barnes PJ, Karin M. Nuclear factor-kappaB: a pivotal transcription factor in chronic inflammatory diseases. *N Engl J Med* 1997;336:1066–71.
39. Bours V, Bonizzi G, Bentires-Alj M et al. NF-kappaB activation in response to toxic and therapeutic agents: role in inflammation and cancer treatment. *Toxicology* 2000;153:27–38.

40. Karin M, Cao Y, Greten FR et al. NF-kappaB in cancer: from innocent bystander to major culprit. *Nat Rev Cancer* 2002;2: 301–10.
41. Yu H, Lin L, Zhang Z et al. Targeting NF- κ B pathway for the therapy of diseases: mechanism and clinical study. *Signal Transduct Target Ther* 2020;5:209.

Biphasic effect of mechanical stress on lymphocyte activation

Mhd Yousuf Yassouf^{1,2}  | Xu Zhang^{1,2} | Zisheng Huang^{1,2} | Da Zhai^{1,2} |
Reiko Sekiya^{1,2} | Tsuyoshi Kawabata^{1,2}  | Tao-Sheng Li^{1,2} 

¹Department of Stem Cell Biology, Nagasaki University Graduate School of Biomedical Sciences, Nagasaki, Japan

²Department of Stem Cell Biology, Atomic Bomb Disease Institute, Nagasaki University, Nagasaki, Japan

Correspondence

Tao-Sheng Li, Department of Stem Cell Biology, Atomic Bomb Disease Institute, Nagasaki University, Sakamoto 1-12-4, Nagasaki 852-8523, Japan.
Email: yosef.yassouf@gmail.com

Funding information

The Collaborative Research Program of the Atomic-bomb Disease Institute of Nagasaki University; A Grant-in-Aid from the Ministry of Education, Science, Sports, Culture and Technology, Japan, Grant/Award Number: 21K19533; Japan Agency for Medical Research and Development, Grant/Award Number: 20Im0203081h0002

Abstract

Mechanical forces can modulate the immune response, mostly described as promoting the activation of immune cells, but the role and mechanism of pathological levels of mechanical stress in lymphocyte activation have not been focused on before. By an *ex vivo* experimental approach, we observed that mechanical stressing of murine spleen lymphocytes with 50 mmHg for 3 h induced the nuclear localization of NFAT1, increased C-Jun, and increased the expression of early activation marker CD69 in resting CD8⁺ cells. Interestingly, 50 mmHg mechanical stressing induced the nuclear localization of NFAT1; but conversely decreased C-Jun and inhibited the expression of CD69 in lymphocytes under lipopolysaccharide or phorbol 12-myristate 13-acetate/ionomycin stimulation. Additionally, we observed similar changes trends when comparing RNA-seq data of hypertensive and normotensive COVID-19 patients. Our results indicate a biphasic effect of mechanical stress on lymphocyte activation, which provides insight into the variety of immune responses in pathologies involving elevated mechanical stress.

KEYWORDS

biphasic effect, immune response, lymphocyte activation, mechanical stress, mechanotransduction

1 | INTRODUCTION

Mechanical forces play an essential role in maintaining the homeostasis of our body. Various mechanical forces, such as shear stress and hydrostatic pressure, are known to regulate the biological properties of cells, especially in the circulatory and immunological systems. In the past decade, mechanosensing and mechanotransduction of cells in response to different mechanical forces have been one of the hottest topics of life science. However, the precise role and relevant molecular mechanism of mechanical forces in the biological properties of tissue cells is still poorly understood because it is extremely difficult to distinguish the mechanical forces from other factors by *in vivo* experimental approach.

Previous studies have explored the mechanical stress-induced responses of different cell types using various mechanical cues, including stretch stress (Coste et al., 2010), shear stress (Ranade et al., 2014), hydrostatic pressure (Solis et al., 2019), and various

degrees of scaffold stiffness (Atcha et al., 2021). Among numerous mechanotransduction key molecules, PIEZO1, a mechanosensitive ion channel, has been focused on recently due to its multiple functions and wide expression in all organs. PIEZO1 has been demonstrated to be essential in cyclical hydrostatic pressure sensing for the proper response of macrophages in case of lung infection (Solis et al., 2019).

The role of mechanical forces and stiffness has been reported in triggering the activation of lymphocytes (Judokusumo et al., 2012; Li et al., 2010; Ma & Finkel, 2010), macrophages (Solis et al., 2019), and myeloid cells (Aykut et al., 2020), suggesting that mechanical cues may promote the activation of immune cells. On the other hand, under pathological conditions, mechanical forces around the tissue cells can be altered dynamically, such as the increased mechanical stress in patients with hypertension. Therefore, it will be possible that elevated hydrostatic pressure induces the activation of circulating leukocytes but may conversely impair their activation and function in

response to severe infections, as clinical studies indicated worse outcomes and severity for hypertensive patients who suffer serious infections (Guan et al., 2020; Piroth et al., 2021; Schoen et al., 2019). Thus, we were interested in investigating the precise role and molecular mechanism of elevated mechanical stress, specifically elevated pathological levels of hydrostatic pressure, in lymphocyte activation as it has not been focused on previously.

2 | MATERIALS AND METHODS

2.1 | Animals and cell culture

C57BL/6 male mice (CLEA), 8–12 weeks old, were used in this study for spleen harvest. The animals were bred in specific, pathogen-free conditions and were allowed free access to food and water in a temperature-controlled environment with a 12:12 h light–dark cycle. All animal procedures were performed in accordance with institutional and national guidelines.

Freshly harvested spleens were cut using a surgical blade then strained against a 70 μm cell strainer using gentle pressure applied by syringe plug while adding phosphate-buffered saline (PBS). Suspended spleen cells were collected, and then red blood cells (RBCs) were lysed using RBC lysis (Invitrogen) according to the manufacturer's instructions. The resulting cells were strained against a 40 μm cell strainer to discard any cell aggregates, then suspended at a density of 5×10^6 cells/ml in RPMI-1640 with L-glutamine (Wako) supplemented with 10% fetal bovine serum (FBS; HyClone FBS; GE Healthcare), 100 U/ml penicillin and 100 $\mu\text{g}/\text{ml}$ streptomycin (Wako), and 50 μM 2-mercaptoethanol (Sigma) at 37°C in a 5% CO_2 -humidified atmosphere, all following treatments were applied after 3 h of cells incubation. In some experiments, lymphocytes were treated with Piezo1 agonist Yoda1 at 10 μM concentration (Cayman Chemical), ROCK inhibitor Y27632 at 10 μM concentration (ATCC), and O55:B5 *Escherichia coli* lipopolysaccharides (LPS) at 1 $\mu\text{g}/\text{ml}$ concentration (Sigma). Cell activation cocktail (phorbol 12-myristate 13-acetate/ionomycin [PMA/I]) was purchased from Bio-Legend and used at the concentrations suggested by the manufacturer (PMA/I: PMA 81 nM, ionomycin 1.34 μM ; reagents are described in Table S1).

2.2 | Mechanical stress

For mechanical stress, culture dishes were subjected to static pressure using a hydrostatic pressure system from STREX (STREX AGP-3001S) which was placed inside a 5% CO_2 cell culture incubator at 37°C (Figure S1). The compressor unit intakes the air from the 5% CO_2 balanced air within the cell culture incubator, then injects it into the sealed chamber. The compressor unit has a sensitive sensor to measure the pressure inside the chamber and adjust it to the value assigned using the controllers on the compressor unit. We used 50 mmHg for the purpose of this experiment.

2.3 | Flow cytometry

Following incubation in the various culture conditions, cells were harvested and directly washed with cold PBS for 5 min at 1400g at 4°C, then 5×10^5 cells from each condition were resuspended in Flow Cytometry Staining Buffer (FACS) buffer (4% FBS, cold PBS) and incubated with Fc block for 15 min, followed by adding conjugated antibodies for CD4, CD8, CD19, and CD69 to each tube and incubated for 30 min at 4°C (dilutions and conjugated fluorochromes are described in Table S2). After staining and washing, cells were suspended in FACS buffer, and data were acquired on BD FACSVerse (BD Biosciences). A minimum of 10,000 cell counts was analyzed.

2.4 | RNA isolation and RT-qPCR

Following incubation in the various culture conditions, cells were harvested and directly washed with cold PBS for 5 min at 1400g at 4°C, then resulting cell pellets were used to isolate total RNA (approximately 10^7 cells in each pellet) using Quick-RNA™ Microprep Kit (Zymo Research) according to manufacturer's instructions. RNA quantity and quality were assessed using NanoDrop™ 2000/2000c (Thermo Fisher Scientific). Complementary DNA (cDNA) was generated using 900 ng of purified total RNA with SuperScript™ VILO™ MasterMix (Invitrogen) according to the manufacturer's instructions. The amplified cDNA was diluted at a ratio of 1:10 in DNase- and RNase-free water. Quantitative reverse transcription polymerase chain reaction were performed using 2 μl cDNA (equivalent to 18 ng total RNA) per reaction with THUNDERBIRD SYBR qPCR Mix (TOYOBO) on LightCycler® 480 Instrument II (Roche Life Science) according to manufacturer's instructions. Fold changes of expression are relative to the control using the $2^{-\Delta\Delta C^t}$ method (Livak & Schmittgen, 2001). Primers sequences are listed in Table S3.

2.5 | Enzyme-linked immunosorbent assay

The levels of interleukin 2 (IL-2), interferon γ (IFN- γ), and tumor necrosis factor α (TNF- α) in supernatants were determined by sandwich enzyme-linked immunosorbent assay (ELISA) using LEGEND MAX™ Mouse IL-2 ELISA Kit, LEGEND MAX™ Mouse IFN- γ ELISA Kit, and LEGEND MAX™ Mouse TNF- α ELISA Kit, respectively (BioLegend) according to manufacturer's instructions. Optical densities were acquired using an iMark Microplate Reader (Bio-Rad).

2.6 | Immunocytochemistry

Following incubation in the various culture conditions, stimulations were stopped by the addition of 10 volumes of ice-cold PBS then cells were pelleted at 1400g at 4°C, and 5×10^5 cells from each

condition were resuspended in FACS buffer (4% FBS, cold PBS) and incubated with Fc block for 15 min, followed by adding conjugated antibodies for CD4, and CD8 to each tube and incubated for 60 min in the dark at 4°C (dilutions and conjugated fluorochromes are described in Table S2). After staining, cells were washed twice and suspended in fixation/permeabilization buffer (Invitrogen) for 60 min in the dark at 4°C, then washed with permeabilization buffer (Invitrogen) two times 5 min each, at 1400g at 4°C, then blocked in 3% bovine serum albumin for 20 min, followed by 60 min incubation in the dark with primary antibodies against NFAT1 (Cell Signaling Technology) or HIF1- α (Novus Biologicals). Cells were washed and incubated with Alexa Fluor 546- or Alexa Fluor 647-conjugated secondary antibodies for 60 min in the dark. After washing, cells were incubated with 4',6-diamidino-2-phenylindole for 30 min in the dark. Stained cells were attached to microscope slides by centrifugation for 3 min at 112.9g using Cytospin 3 (Thermo Shandon) followed by adding a Vectashield Vibrance mounting medium (Vector Laboratories) and coverslips. The cells were viewed using a $\times 63$ oil-immersion objective lens on LSM 800 confocal microscope (Zeiss). Fluorescent image analysis for quantification and localization estimates were performed with the NIH ImageJ software package using the same image analysis workflow for all images in all replicates.

2.7 | RNA sequencing data set analysis

The RNA sequencing raw data were downloaded from the gene expression omnibus (GEO) database (Barrett et al., 2013) with accession number GSE157859 (Zheng et al., 2020). GSE157859 included RNA sequencing data prepared from peripheral venous blood samples of patients with COVID-19 which were obtained at different clinical stages. Among those patients, four patients have hypertension as the only main comorbidity (hypertensive patients: HT), and we selected four closest matching patients with no comorbidities as a control group (normotensive patients: NT), we compared the data from four HT patients (GSM4776962, GSM4776976, GSM4776981, GSM4776985) with four NT patients (GSM4776954, GSM4776964, GSM4776967, GSM4776974) in the treatment clinical-stage, also in the rehabilitation stage 2 HT patients (GSM4776978, GSM4776987) with three NT patients (GSM4776956, GSM4776966, GSM4776969) data were available for comparison. The raw sequencing data were uploaded to the Galaxy web platform, and we used the public server at usegalaxy.org to analyze the data (Afgan et al., 2016). Quality of data were checked by FastQC v0.11.8 (Andrews, 2010) followed by Adapters removal, reads trimming, and quality filtering using Fastp v0.20.1 (Chen et al., 2018). The clean reads were then aligned to the primary assembly of the human reference genome, GRCh38, using HISAT2 v2.1.0 (Kim et al., 2015). We used featureCounts v2.0.1 (Liao et al., 2014) to count RNA-seq reads for genes with GRCh38 annotation. Finally, edgeR v3.24.1 (Robinson et al., 2010) was used to perform differential expression testing and estimate log₂ fold change [HT-NT].

2.8 | Statistical analysis

All results are presented as the means \pm SD. Statistical significance between two groups was determined using a *t*-test. Differences were considered significant when two-sided $p < 0.05$.

3 | RESULTS

3.1 | Mechanical stress enhances CD69 expression in resting CD8+ cells, but conversely impairs the activation of lymphocytes under LPS or PMA/I stimulation

Lymphocytes were collected from the mouse spleen and then incubated without (Resting) or with the addition of LPS or PMA/I in medium (stimulated). To investigate the potential effect of mechanical stress on lymphocyte activation, we used a bioreactor capable of subjecting cells to 50 mmHg pressure for 3 h, and as a control, cells were placed in the atmospheric pressure, both inside a 5% CO₂ incubator at 37°C (Figure S1). We evaluated the expression of the early activation marker CD69 using flow cytometry. In resting lymphocytes, mechanical stress significantly increased the expression of CD69 in CD8+ T cells (31.8 ± 3.2 vs. 22.78 ± 1.95 ; $p < 0.01$; Figure 1a). However, with the addition of LPS in the medium, mechanical stress significantly decreased the expression of CD69 in CD19+ B cells (2841 ± 1178 vs. 5177 ± 1570 ; $p < 0.01$; Figure 1a). Similarly, under the stimulation with PMA/I, mechanical stress significantly decreased the expression of CD69 in CD4+ T cells (9188 ± 855.5 vs. 18461 ± 1455 ; $p < 0.01$; Figure 1a), CD8+ T cells (9314 ± 753.5 vs. 22499 ± 1453 ; $p < 0.01$; Figure 1a), and CD19+ B cells (13642 ± 3789 vs. 16227 ± 3497 ; $p = 0.02$; Figure 1a). CD19+ B cells respond to LPS stimulation because of the TLR4 receptor on murine B cells recognizing LPS. On the other hand, murine CD4+ and CD8+ T cells do not respond to LPS due to the absence of the TLR4 receptor (Applequist et al., 2002).

We also evaluated the messenger RNA (mRNA) expression of several major cytokines using RT-qPCR. In resting lymphocytes, mechanical stress significantly decreased the mRNA level of *Il2* ($p < 0.01$; Figure 1b), but increased the mRNA level of *Ifng* ($p = 0.06$; Figure 1b). Interestingly, with the addition of LPS in medium, mechanical stress significantly decreased the mRNA levels of *Il1b* ($p = 0.01$; Figure 1b), *Il2* ($p = 0.09$; Figure 1b), and *Il10* ($p = 0.02$; Figure 1b). Similarly, under PMA/I stimulation, mechanical stress significantly decreased the mRNA levels of *Ifng* ($p < 0.01$; Figure 1b), *Il2* ($p = 0.01$; Figure 1b), *Il4* ($p = 0.03$; Figure 1b), and *Il10* ($p < 0.01$; Figure 1b), while increased the mRNA level of *Tnf* ($p = 0.02$; Figure 1b).

To further confirm our findings, we measured the protein levels of IFN- γ , IL-2, and TNF- α in the culture medium using ELISA. In resting lymphocytes, mechanical stress only slightly increased the secretion of IFN- γ ($p = 0.056$; Figure 1c). However, for PMA/I-stimulated lymphocytes, mechanical stress significantly decreased

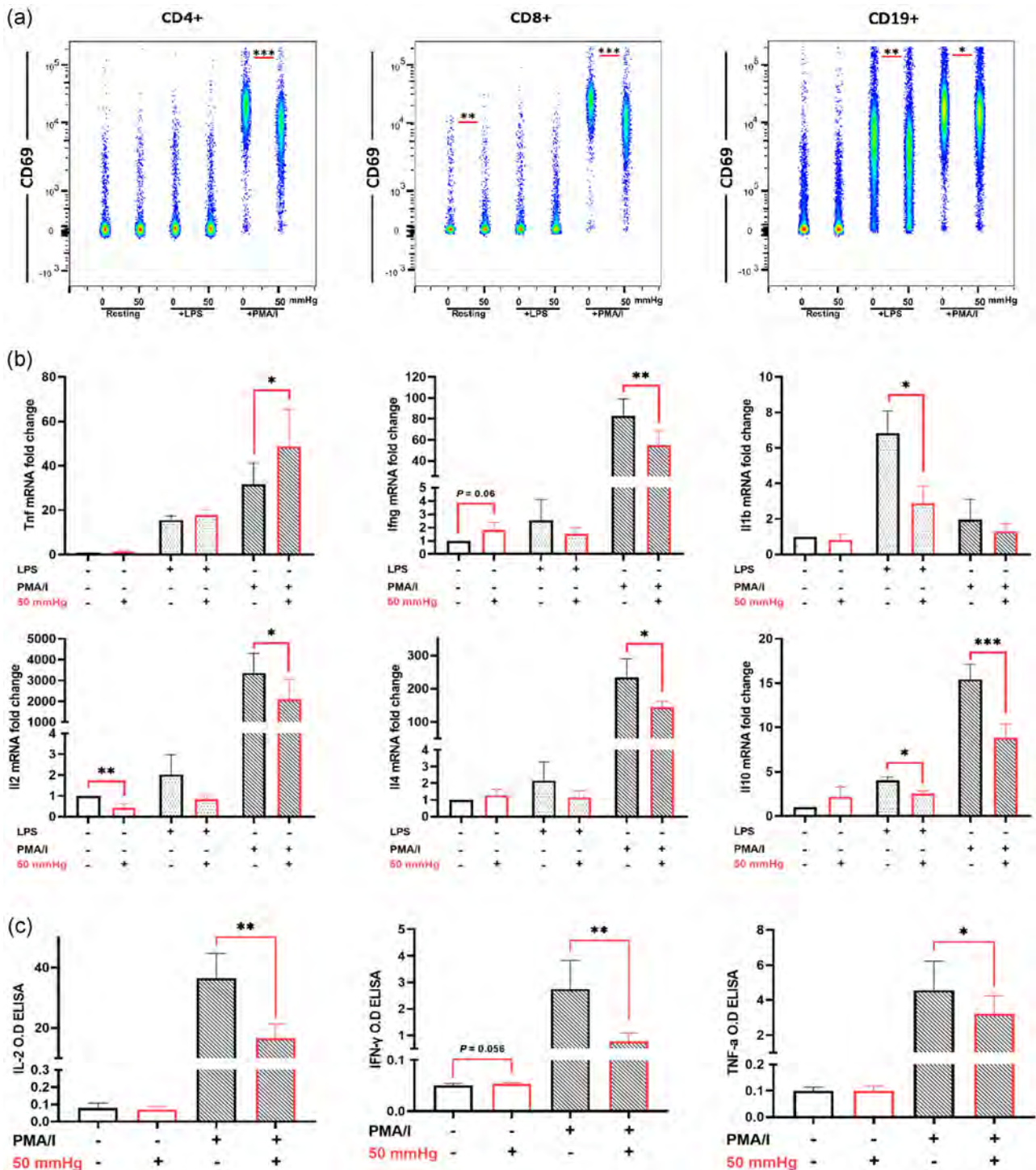


FIGURE 1 The expression of the activation marker CD69 and cytokines in lymphocytes following mechanical stressing. (a) Flow cytometry analysis on CD69 expression among CD4+, CD8+, and CD19+ cells following LPS, or PMA/I stimulation compared to resting lymphocytes. Pseudocolored plots indicating mechanical stressing effect, and data represent the results of four independent experiments. (b) Bar graphs indicating a mechanical stressing effect on mRNA fold changes of *Tnf*, *Ifng*, *Il1b*, *Il2*, *Il4*, *Il10* in lymphocytes following LPS, or PMA/I stimulation compared to resting lymphocytes (data represent the results of four independent experiments, mRNA fold changes are calculated to the control $2^{-\Delta\Delta C_t}$). (c) Bar graphs indicating a mechanical stressing effect on IL-2, IFN- γ , and TNF- α levels as evaluated by ELISA assay in the culture medium of PMA/I-stimulated lymphocytes compared to resting lymphocytes (figures represent the results of six independent experiments, data are represented as mean \pm SD); (mechanical stressing: 50 mmHg/3 h). ELISA, enzyme-linked immunosorbent assay; IFN- γ , interferon γ ; IL-2, interleukin 2; LPS, lipopolysaccharide; MFI, median fluorescence intensity; mmHg, millimeter of mercury; mRNA, messenger RNA; PMA/I, phorbol myristate acetate/ionomycin; TNF- α , tumor necrosis factor α . * p \leq 0.05, ** p \leq 0.01, *** p \leq 0.001

the secretion of IFN- γ ($p < 0.01$; Figure 1c), IL-2 ($p < 0.01$; Figure 1c), and TNF- α ($p = 0.01$; Figure 1c).

IL-2 is usually secreted from activated CD4 $^{+}$ and CD8 $^{+}$ T cells. According to our data, mechanical stress decreased the mRNA expression of *Il2* in both resting and PMA/I-stimulated lymphocytes but induced CD69 expression in resting CD8 $^{+}$ cells. We speculated that the expression change in IL-2 might be related to the effect of mechanical stress on CD4 $^{+}$ T cells. Therefore, mechanical stress may promote the activation of resting CD8 $^{+}$ T cells, but likely shows an inhibitory effect on lymphocyte activation under the stimulation with PMA/I or LPS.

3.2 | RhoA/ROCK pathway and PIEZO1 are not closely involved in the mechanical stress-induced inhibition on the activation of PMA/I-stimulated lymphocytes

Previous studies have described that the cellular response to mechanical forces is regulated through RhoA/ROCK pathway (Boyle et al., 2020; Takemoto et al., 2015; Teramura et al., 2012), and ROCK inhibition has been demonstrated to suppress lymphocyte activation (Aihara et al., 2003; Lou et al., 2001; Tharaux et al., 2003). Therefore, we investigated whether mechanical stress inhibited lymphocyte

activation through RhoA/ROCK pathway. We incubated lymphocytes with or without Y27632, a ROCK inhibitor, at 10 μ M as previous studies suggest this concentration to show its maximum effects (Aihara et al., 2003; Bardi et al., 2003). Unexpectedly, ROCK inhibition did not obviously mitigate the mechanical stress-induced changes in the expression of CD69 in PMA/I-stimulated lymphocytes (Figure S2a), as well as their secretion of IFN- γ , IL-2, and TNF- α . Instead, ROCK inhibition even enhanced the inhibition in some of these parameters (Figure S2b). Therefore, the RhoA/ROCK pathway might not be closely involved in the mechanical stress-induced inhibition of lymphocyte activation under PMA/I stimulation.

Studies have also focused on the role of PIEZO1 in the function and activation of myeloid cells (Aykut et al., 2020), macrophages (Solis et al., 2019), T lymphocytes (Liu et al., 2018). BioGPS gene portal data also showed that murine T lymphocytes express considerable amounts of PIEZO1 similar to macrophages (Figure S3; Lattin et al., 2008; Wu et al., 2009). Thus, we investigated whether PIEZO1 is involved in the observed effects of mechanical stress on lymphocyte activation. We incubated resting and PMA/I-stimulated lymphocytes with or without Yoda1, a PIEZO1 agonist, for 3 h followed by evaluations. For resting lymphocytes, Yoda1 significantly increased the expression of CD69 in CD8 $^{+}$ T cells ($p < 0.01$; Figure 2a). For PMA/I-stimulated lymphocytes, Yoda1 conversely decreased CD69 expression in CD4 $^{+}$ T cells ($p < 0.01$; Figure 2a) and

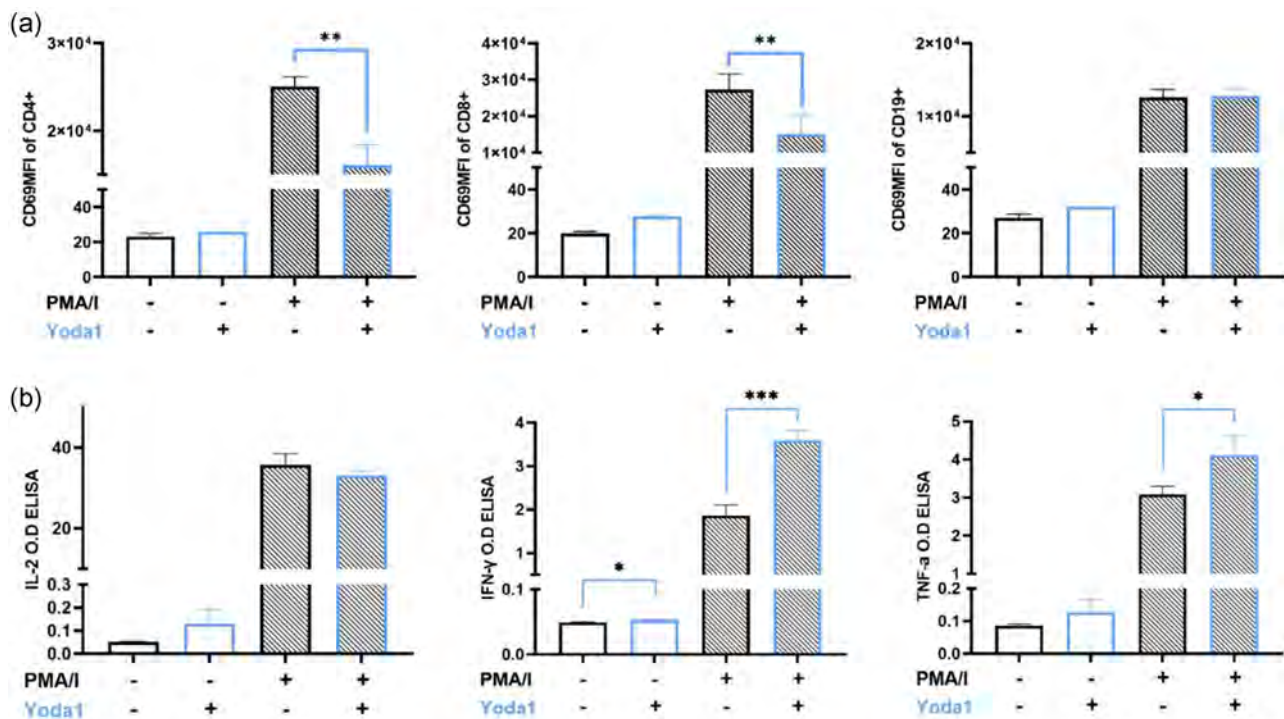


FIGURE 2 The expression of the activation marker CD69 and cytokines in lymphocytes following PIEZO1 activation using Yoda1. (a) Flow cytometry analysis on CD69 expression among CD4 $^{+}$, CD8 $^{+}$, and CD19 $^{+}$ cells following PMA/I and Yoda1 treatments. (b) Bar graphs indicating Yoda1 effect on IL-2, IFN- γ , and TNF- α levels as evaluated by ELISA assay in the culture medium of PMA/I-stimulated lymphocytes compared to resting lymphocytes. (Data represent the results of three independent experiments, data are represented as mean \pm SD); (Yoda1: 10 μ M/3 h). ELISA, enzyme-linked immunosorbent assay; IFN- γ , interferon γ ; IL-2, interleukin 2; MFI, median fluorescence intensity; OD, optical density; PMA/I, phorbol myristate acetate/Ionomycin; TNF- α , tumor necrosis factor α . * $p \leq 0.05$, ** $p \leq 0.01$

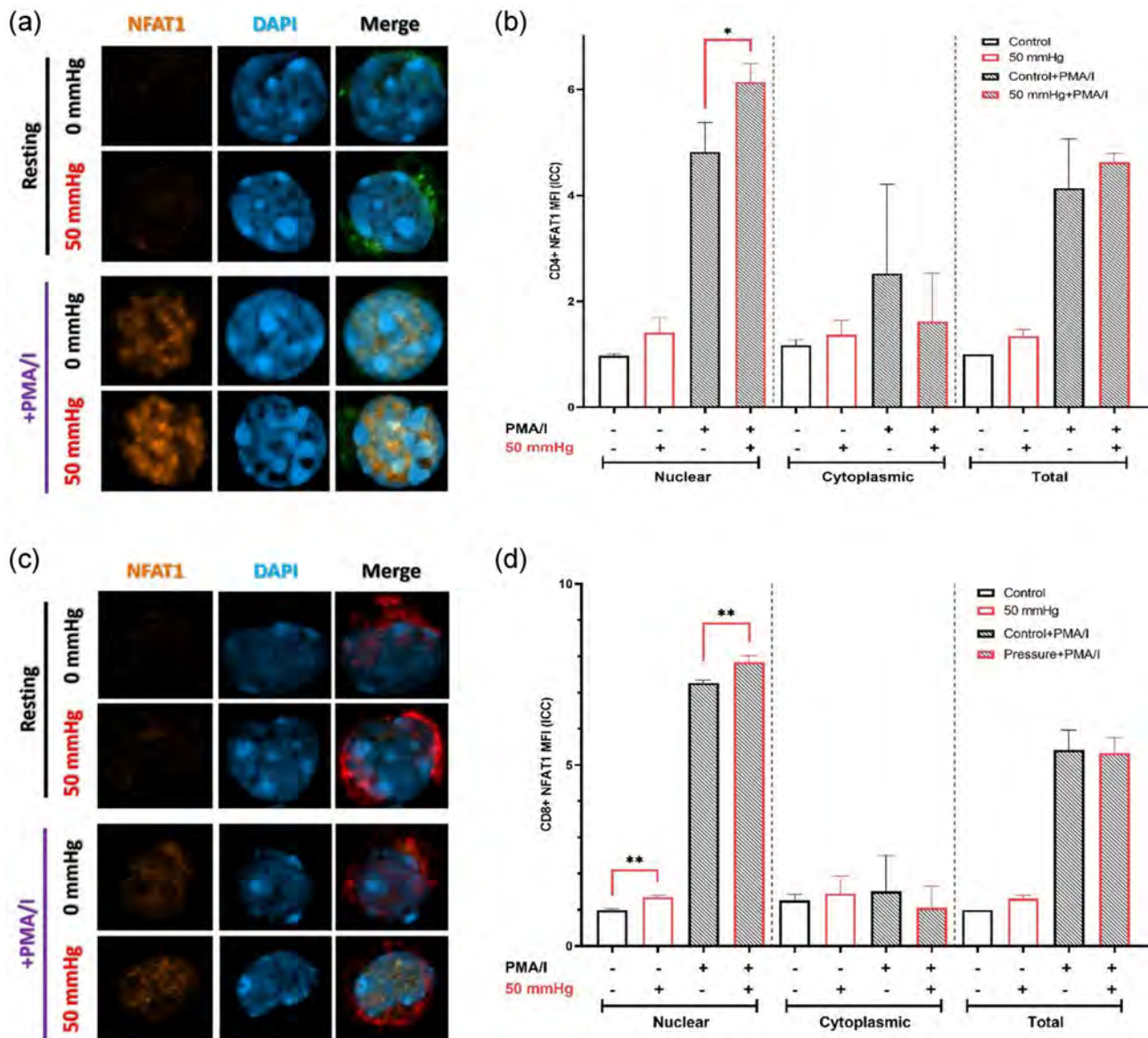


FIGURE 3 NFAT1 expression changes in lymphocytes following mechanical stressing. (a) NFAT1 expression changes in CD4+ cells following PMA/I stimulation and mechanical stressing (Yellow = NFAT1, Cyan = DAPI, Green = CD4). (b) Bar graphs indicating the nuclear, cytoplasmic, and total relative expression changes of NFAT1 in CD4+ cells. (c) NFAT1 expression changes in CD8+ cells following PMA/I stimulation and mechanical stressing (Yellow = NFAT1, Cyan = DAPI, Red = CD8). (d) Bar graphs indicate the relative expression of NFAT1 in CD8+ cells in the nucleus, cytoplasm, and total cell. (Mechanical stressing: 50 mmHg/3 h). (Data represent the results of three independent experiments, data are represented as mean \pm SD). DAPI, 4',6-diamidino-2-phenylindole; MFI, mean fluorescence intensity; mmHg, millimeter of mercury; PMA/I, phorbol myristate acetate/ionomycin. * $p \leq 0.05$, ** $p \leq 0.01$

CD8+ T cells ($p < 0.01$; Figure 2a), but did not significantly change CD69 expression in CD19+ B cells (Figure 2a).

ELISA testing of culture medium showed that Yoda1 slightly induced the secretion of IFN- γ from resting lymphocytes ($p = 0.02$; Figure 2b). Differed from mechanical stress, Yoda1 did not change the secretion of IL-2 but increased the secretion of IFN- γ ($p \leq 0.01$; Figure 2a) and TNF-TNF- α ($p = 0.03$; Figure 2b) from PMA/I-stimulated lymphocytes. PIEZO1 agonist and mechanical stress significantly and very similarly promoted CD69 expression in resting CD8+ cells and inhibited CD69 expression in PMA/I-stimulated lymphocytes, however, they intriguingly showed opposite effects on

cytokine secretion. This suggests that mechanisms other than PIEZO1 mechanosensing by which mechanical stress inhibits the secretion of cytokines from PMA/I-stimulated lymphocytes.

3.3 | Mechanical stress promotes nuclear HIF1- α localization in resting but not PMA/I-stimulated lymphocytes

It has been reported that mechanical loading induces HIF1- α expression and nuclear localization (Jing et al., 2020). Several previous

studies have also reported an increased expression of HIF1- α in activated T lymphocytes (Nicoli et al., 2018; Wang et al., 2011) and mast cells (Walczak-Drzewiecka et al., 2008). As the enhanced activity of HIF1- α may promote the effector function of CD8+ T cells (Palazon et al., 2014), we measured HIF1- α expression and localization. We incubated resting and PMA/I-stimulated murine spleen lymphocytes with or without 50 mmHg mechanical stressing for 3 h. In resting lymphocytes, mechanical stress induced the nuclear localization of HIF1- α in both CD4+ and CD8+ T cells (Figure S4). PMA/I-stimulated lymphocytes expressed higher HIF1- α compared to resting ones. In PMA/I-stimulated lymphocytes, there was no significant difference between mechanically stressed or not, although PMA/I-stimulated CD8+ lymphocytes tend to have decreased nuclear HIF1- α under mechanical stress (Figure S4). Mechanical stress did not change the mRNA levels of *Hif1a* in resting lymphocytes but was shown to inhibit the enhancement of *Hif1a* expression in PMA/I-stimulated lymphocytes ($p = 0.095$; Figure S5). Based on our results, mechanical stress induced HIF1- α nuclear localization in resting lymphocytes, but conversely inhibited the enhancement of *Hif1a* mRNA expression in PMA/I-stimulated lymphocytes, supporting the inhibitory effect of mechanical stress in PMA/I-stimulated lymphocytes.

3.4 | Mechanical stress induces NFAT1 nuclear localization but reduces Jun expression in PMA/I-stimulated lymphocytes

It is well known that increased mechanical stress can increase intracellular Ca^{2+} levels (Hamill & Martinac, 2001). Increased calcium levels within the cytoplasm of T lymphocytes lead to the dephosphorylation of NFAT followed by its nuclear localization to initiate the transcription program (McCaffrey et al., 1993; Northrop et al.,

1994). Thus, we tried to investigate whether NFAT1 is involved in the inhibitory effect of mechanical stress on the activation of PMA/I-stimulated lymphocytes. In resting lymphocytes, mechanical stress exactly increased the nuclear levels of NFAT1 in both CD4+ and CD8+ cells (Figure 3). Similarly, for PMA/I-stimulated lymphocytes, mechanical stress also induced the nuclear localization of NFAT1 in both CD4+ and CD8+ cells (Figure 3).

NFAT1 nuclear localization might initiate either T lymphocyte activation or energy, depending on the availability of other transcription factors such as AP1 (Hogan, 2017; Macián et al., 2002). Cooperation of NFAT with AP-1 (C-Jun: C-Fos) is essential for proper activation of lymphocytes, thus we further investigated the expression of AP-1. In resting lymphocytes, mechanical stress significantly increased the mRNA level of *Jun* ($p = 0.02$; Figure 4). Conversely, under PMA/I stimulation, mechanical stress significantly decreased mRNA levels of *Jun* ($p = 0.04$; Figure 4). While mechanical stress did not alter *Fos* mRNA levels in either resting or PMA/I-stimulated lymphocytes. As mechanical stress showed to promote NFAT1 nuclear localization but to decrease *Jun* expression in PMA/I-stimulated lymphocytes, mechanical stress may suppress *Jun* to impair the activation of PMA/I-stimulated lymphocytes.

3.5 | Hypertensive COVID-19 patients have altered JUN and CD69 expression

Hypertension imposes circulating leukocytes to elevated hydrostatic pressure. Clinical studies have reported the worse outcome of infections in patients with hypertension than those without (Guan et al., 2020; Piroth et al., 2021; Schoen et al., 2019). Out of 165 hypertensive COVID-19 patients, 41 (24.85%) patients have developed severe symptoms, while of the 495 COVID-19 patients without comorbidities, only 10 (2.02%) patients were severe cases

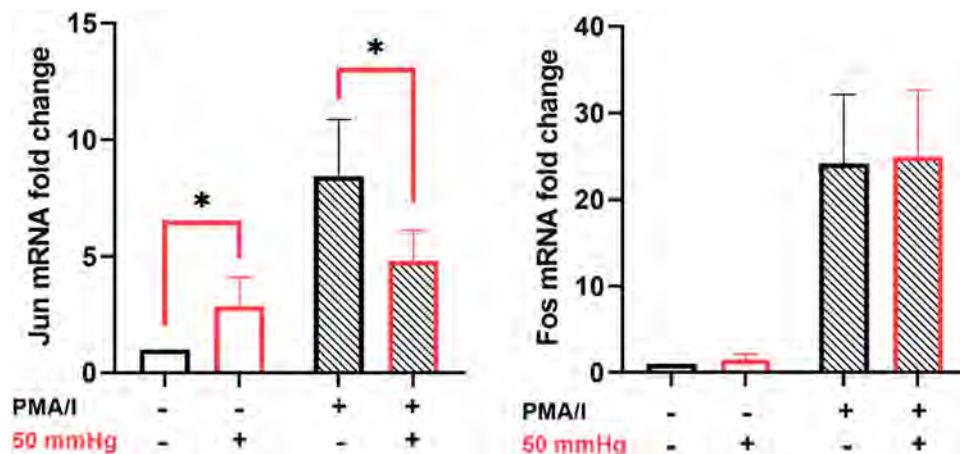


FIGURE 4 *Jun* and *Fos* mRNA expression changes following mechanical stressing in lymphocytes. Bar graphs indicating mechanical stressing effect on mRNA expression changes of *Jun* and *Fos* in PMA/I-stimulated lymphocytes compared to resting lymphocytes (data represent the results of four independent experiments, mRNA fold changes are calculated to the control $2^{-\Delta\Delta C_t}$, data are represented as mean \pm SD); (mechanical stressing: 50 mmHg/3 h). mmHg, millimeter of mercury; mRNA, messenger RNA; PMA/I, phorbol myristate acetate/ionomycin. * $p \leq 0.05$

(Guan et al., 2020). Another study has found that out of the patients hospitalized for COVID-19 and seasonal influenza, 33.1% and 28.2% of cases, respectively, have the comorbidity of hypertension (Piroth et al., 2021). Additionally, it has been found that the presence of hypertension on hospital admission was associated with worse clinical outcomes in patients with H1N1 influenza A virus infection (Schoen et al., 2019). Therefore, we were interested in searching whether lymphocyte activation-related genes are associated with the development of severe symptoms in hypertensive COVID-19 patients. We analyzed RNA sequencing data prepared from PBMC of COVID-19 patients with hypertension or without. PBMCs were collected at the treatment stage (15.9 ± 8.1 days after infection day) and rehabilitation stage (67.2 ± 6.4 days after infection day), probably similar to the stimulated lymphocytes and resting lymphocytes, respectively (Zheng et al., 2020). Results show that, in the treatment stage, hypertensive COVID-19 patients (HT) have reduced *JUN* and *CD69* expression compared to normotensive COVID-19 patients (NT) (Figure 5). Conversely, in the rehabilitation stage, hypertensive patients have higher *JUN*, *FOS*, *CD69*, and *TNF* expression compared with normotensive ones (Figure 5). These results suggest the likely relationship between *JUN* expression and lymphocyte activation changes in hypertensive patients. Therefore, we speculate that

hypertensive patients may have impaired immune responses to serious infections, like the COVID-19.

4 | DISCUSSION

In this study, we investigated the effect of elevated mechanical stress in lymphocyte activation by an ex vivo experimental approach. We mechanically stressed murine spleen lymphocytes with 50 mmHg either in the resting state (no-stimulation) or in LPS- or PMA/I-stimulated state. Our data indicated that mechanical stress induced *CD69* expression of resting *CD8+* cells but conversely impaired lymphocyte activation under the LPS or PMA/I stimulation. Based on our ex vivo experimental data, it seems that mechanical stress can induce the activation of resting lymphocytes but may conversely impair lymphocyte activation when responding to exogenous stimulations or severe infections.

In searching for mechanotransduction key molecule(s) involved in the observed biphasic effects of mechanical stress on lymphocyte activation, we found that RhoA/ROCK pathway might not be closely involved in the mechanical stress-induced inhibition of lymphocyte activation under PMA/I stimulation. Liu et al. (2018) showed that

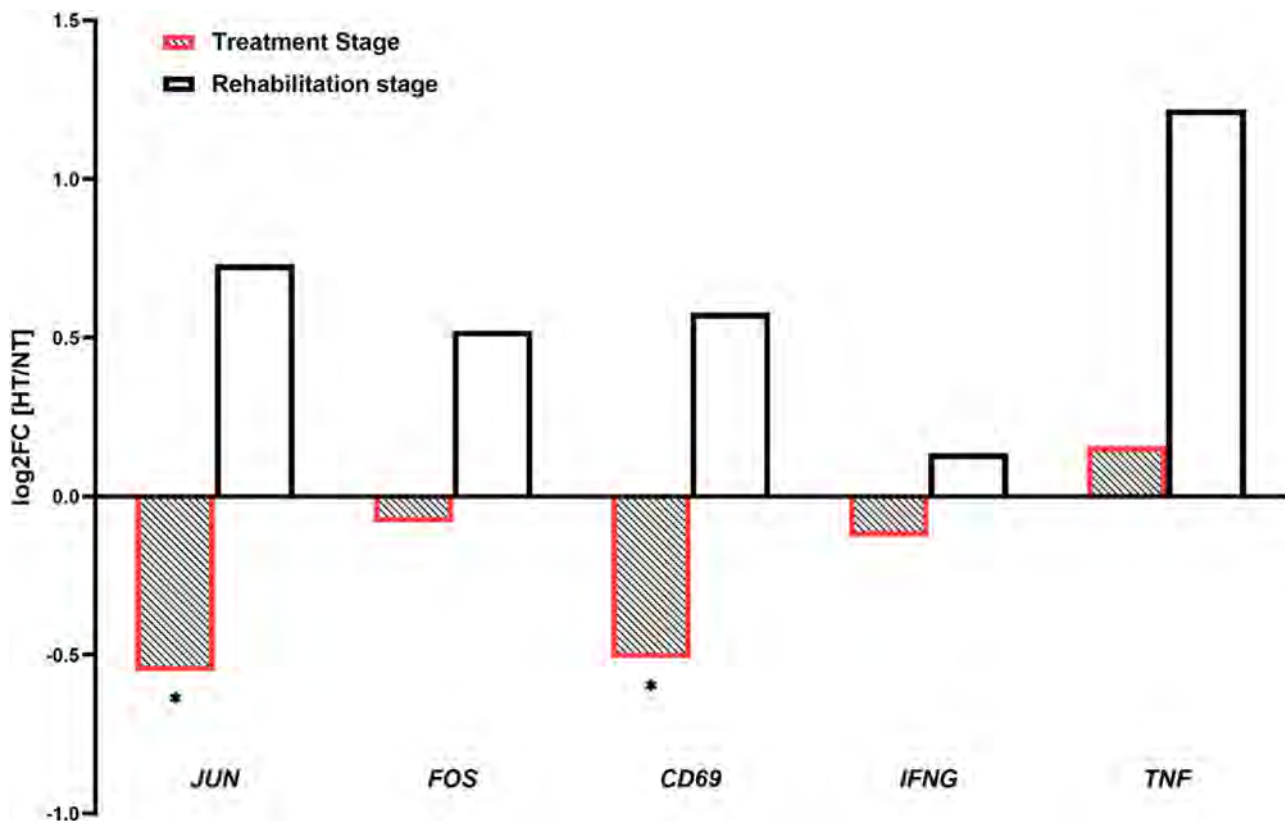


FIGURE 5 Hypertension comorbidity effect on the expression of lymphocyte activation-related genes in peripheral blood mononuclear cells from COVID-19 patients. Bar graphs indicate log₂FC changes for the expression of *JUN*, *FOS*, *CD69*, *IFNG*, and *TNF* when comparing hypertensive COVID-19 patients (HT) to normotensive COVID-19 patients (NT) in both the treatment stage and rehabilitation stage. (Treatment stage comparison include four HT patients and four NT patients; rehabilitation stage comparison include two HT patients and three NT patients); log₂FC = edgeR Log₂ fold change. HT, hypertensive patients; NT, normotensive patients. * $p \leq 0.05$ (edgeR p -value)

Yoda1, PIEZO1 agonist, rescued the activation and CD69 expression of CD4+ and CD8+ T cells treated with soluble anti-CD3/anti-CD28 Abs, however in that study, the single effect of Yoda1 treatment was not explained, nor the effect of Yoda1 addition to properly activated T cells (Liu et al., 2018). While, in this study, we showed a similar effect of Yoda1 and mechanical stress on CD69 expression, where both promote its expression in resting CD8+ cells and reduce it in PMA/I-stimulated lymphocytes. However, cytokines expression profiles of PMA/I-stimulated lymphocytes were interestingly different between PIEZO1 agonist Yoda1 and mechanical stress. PIEZO1 agonist promoted IFN- γ and TNF- α secretion which agrees with the enhanced inflammatory activation by Yoda1 in IFN- γ /LPS stimulated macrophages (Atcha et al., 2021), but mechanical stress conversely inhibited their secretion along with IL-2, suggesting that mechanisms other than PIEZO1 mechanosensing by which mechanical stress inhibits the expression of cytokines in PMA/I-stimulated lymphocytes. Additionally, we found that mechanical stress may alter HIF1- α nuclear localization and levels in a trend going along with the biphasic effect of mechanical stress in lymphocyte activation.

Mechanical stress may increase intracellular Ca²⁺ levels (Hamill & Martinac, 2001), and the increased cytoplasm Ca²⁺ levels in T-lymphocytes can lead to NFAT nuclear localization (McCaffrey et al., 1993; Northrop et al., 1994). We found that mechanical stress promoted NFAT1 nuclear localization in both resting and PMA/I-stimulated lymphocytes. On the other hand, mechanical stress increased Jun expression in resting lymphocytes but decreased Jun expression in PMA/I-stimulated lymphocytes. As C-Jun cooperation with NFAT is known to be essential for the proper activation of T-lymphocytes (Hogan, 2017; Macián et al., 2002), the alteration of *Jun* expression may provide a reasonable explanation of the different effects of mechanical stress on lymphocyte activation, as observed in our study. With the mechanical stress, enhanced *Jun* may induce the activation in resting CD8+ lymphocytes, while the imbalance between NFAT1 and *Jun* can suppress the activation of lymphocytes in response to PMA/I stimulation.

Considering the clinical relevance of our finding from ex vivo experiments, especially at the lasting pandemic situation of COVID-19, we analyzed RNA-seq data from both hypertensive and normotensive COVID-19 patients. At the treatment stage, hypertensive COVID-19 patients have reduced *JUN* and *CD69* expression compared to normotensive ones, and the opposite at the rehabilitation stage. Interestingly, C-Jun which is an important transcription factor to promote the activation program of lymphocytes mediated by NFAT1 nuclear localization is reduced in hypertensive COVID-19 patients at the treatment stage and conversely increased at the rehabilitation stage. This observation directed us to evaluate C-Jun and C-Fos expression in our experimental setup where we surprisingly found the same trend of *Jun* changes in mechanically stressed murine lymphocytes. *Jun* was described as one of the immediate-early genes in response to mechanical stress in cardiac myocytes (Komuro & Yazaki, 1993; Sadoshima & Izumo, 1997), but for lymphocytes, our study is the first report for the different effects of mechanical stress on *Jun* expression between resting and PMA/I-stimulated lymphocytes.

Biphasic response of T cells spreading-behavior to substrate stiffness has been described (Wahl et al., 2019), where high stiffness leads to either increased or decreased T-cell spreading depending on whether the substrate is functionalized with both anti-CD3 and ICAM-1 or with anti-CD3 only, respectively. The biphasic response of T cells spreading behavior to substrate stiffness may indirectly support the observed biphasic response of lymphocytes to mechanical stress in our study, as T-cell spreading is important for their activation.

Our experimental results provide direct evidence about the biphasic effect of mechanical stress in lymphocyte activation. As mechanical stress will be commonly elevated in various pathological conditions, findings from this study provide novel mechanistic insight into the increased risk of serious infection in individuals with comorbidities involving increased mechanical stress, such as hypertension and diabetes mellitus.

ACKNOWLEDGMENTS

This study was supported by the Collaborative Research Program of the Atomic Bomb Disease Institute of Nagasaki University (to Mhd Yousuf Yassouf and Tao-Sheng Li). Japan Agency for Medical Research and Development (20Im0203081h0002 to Tao-Sheng Li). A Grant-in-Aid from the Ministry of Education, Science, Sports, Culture and Technology, Japan (Grant No. 21K19533 to Tao-Sheng Li).

CONFLICT OF INTERESTS

The authors declare that there are no conflicts of interest.

AUTHOR CONTRIBUTIONS

Conceptualization: Tao-Sheng Li and Mhd Yousuf Yassouf. *Methodology:* Mhd Yousuf Yassouf, Xu Zhang, Zisheng Huang, Da Zhai, Reiko Sekiya, Tsuyoshi Kawabata, Tao-Sheng Li. *Investigation:* Mhd Yousuf Yassouf and Tao-Sheng Li. *Visualization:* Mhd Yousuf Yassouf and Tao-Sheng Li. *Supervision:* Tao-Sheng Li. *Writing—original draft:* Mhd Yousuf Yassouf and Tao-Sheng Li. *Writing—review & editing:* Mhd Yousuf Yassouf and Tao-Sheng Li.

ORCID

Mhd Yousuf Yassouf  <https://orcid.org/0000-0001-7196-9503>

Tsuyoshi Kawabata  <https://orcid.org/0000-0003-0899-0750>

Tao-Sheng Li  <http://orcid.org/0000-0002-7653-8873>

REFERENCES

- Afgan, E., Baker, D., van den Beek, M., Blankenberg, D., Bouvier, D., Čech, M., & Goecks, J. (2016). The Galaxy platform for accessible, reproducible and collaborative biomedical analyses: 2016 update. *Nucleic Acids Research*, 44(W1), W3–W10. <https://doi.org/10.1093/nar/gkw343>
- Aihara, M., Dobashi, K., Iizuka, K., Nakazawa, T., & Mori, M. (2003). Comparison of effects of Y-27632 and isoproterenol on release of cytokines from human peripheral T cells. *International Immunopharmacology*, 3(12), 1619–1625. [https://doi.org/10.1016/S1567-5769\(03\)00184-x](https://doi.org/10.1016/S1567-5769(03)00184-x)
- Andrews, S. (2010). FastQC. A quality control tool for high throughput sequence data.

- Applequist, S. E., Wallin, R. P., & Ljunggren, H. G. (2002). Variable expression of Toll-like receptor in murine innate and adaptive immune cell lines. *International Immunology*, 14(9), 1065–1074. <https://doi.org/10.1093/intimm/14/9/1065>
- Atcha, H., Jairaman, A., Holt, J. R., Meli, V. S., Nagalla, R. R., Veerasubramanian, P. K., & Liu, W. F. (2021). Mechanically activated ion channel Piezo1 modulates macrophage polarization and stiffness sensing. *Nature Communications*, 12(1), 3256. <https://doi.org/10.1038/s41467-021-23482-5>
- Aykut, B., Chen, R., Kim, J. I., Wu, D., Shadaloey, S. A. A., Abengozar, R., & Miller, G. (2020). Targeting Piezo1 unleashes innate immunity against cancer and infectious disease. *Science Immunology*, 5(50), 1–12. <https://doi.org/10.1126/sciimmunol.abb5168>
- Bardi, G., Niggli, V., & Loetscher, P. (2003). Rho kinase is required for CCR7-mediated polarization and chemotaxis of T lymphocytes. *FEBS Letters*, 542(1–3), 79–83. [https://doi.org/10.1016/s0014-5793\(03\)00351-x](https://doi.org/10.1016/s0014-5793(03)00351-x)
- Barrett, T., Wilhite, S. E., Ledoux, P., Evangelista, C., Kim, I. F., Tomashevsky, M., & Soboleva, A. (2013). NCBI GEO: Archive for functional genomics data sets—update. *Nucleic Acids Research*, 41, D991–D995. <https://doi.org/10.1093/nar/gks1193>
- Boyle, S. T., Kular, J., Nobis, M., Ruskiewicz, A., Timpson, P., & Samuel, M. S. (2020). Acute compressive stress activates RHO/ROCK-mediated cellular processes. *Small GTPases*, 11(5), 354–370. <https://doi.org/10.1080/21541248.2017.1413496>
- Chen, S., Zhou, Y., Chen, Y., & Gu, J. (2018). fastp: An ultra-fast all-in-one FASTQ preprocessor. *Bioinformatics*, 34(17), i884–i890. <https://doi.org/10.1093/bioinformatics/bty560>
- Coste, B., Mathur, J., Schmidt, M., Earley, T. J., Ranade, S., Petrus, M. J., & Patapoutian, A. (2010). Piezo1 and Piezo2 are essential components of distinct mechanically activated cation channels. *Science*, 330(6000), 55–60. <https://doi.org/10.1126/science.1193270>
- Guan, W.-J., Ni, Z.-Y., Hu, Y., Liang, W.-H., Ou, C.-Q., He, J.-X., & Zhong, N.-S. (2020). Clinical characteristics of coronavirus disease 2019 in China. *New England Journal of Medicine*, 382(18), 1708–1720. <https://doi.org/10.1056/NEJMoa2002032>
- Hamill, O. P., & Martinac, B. (2001). Molecular basis of mechanotransduction in living cells. *Physiological Reviews*, 81(2), 685–740. <https://doi.org/10.1152/physrev.2001.81.2.685>
- Hogan, P. G. (2017). Calcium-NFAT transcriptional signalling in T cell activation and T cell exhaustion. *Cell Calcium*, 63, 66–69. <https://doi.org/10.1016/j.ceca.2017.01.014>
- Jing, X., Yang, X., Zhang, W., Wang, S., Cui, X., Du, T., & Li, T. (2020). Mechanical loading induces HIF-1 α expression in chondrocytes via YAP. *Biotechnology Letters*, 42(9), 1645–1654. <https://doi.org/10.1007/s10529-020-02910-4>
- Judokusumo, E., Tabdanov, E., Kumari, S., Dustin, M. L., & Kam, L. C. (2012). Mechanosensing in T lymphocyte activation. *Biophysical Journal*, 102(2), L5–L7. <https://doi.org/10.1016/j.bpj.2011.12.011>
- Kim, D., Langmead, B., & Salzberg, S. L. (2015). HISAT: A fast spliced aligner with low memory requirements. *Nature Methods*, 12(4), 357–360. <https://doi.org/10.1038/nmeth.3317>
- Komuro, I., & Yazaki, Y. (1993). Control of cardiac gene expression by mechanical stress. *Annual Review of Physiology*, 55, 55–75. <https://doi.org/10.1146/annurev.ph.55.030193.000415>
- Lattin, J. E., Schroder, K., Su, A. I., Walker, J. R., Zhang, J., Wiltshire, T., & Sweet, M. J. (2008). Expression analysis of G protein-coupled receptors in mouse macrophages. *Immune Research*, 4, 5. <https://doi.org/10.1186/1745-7580-4-5>
- Li, Y.-C., Chen, B.-M., Wu, P.-C., Cheng, T.-L., Kao, L.-S., Tao, M.-H., & Roffler, S. R. (2010). Cutting edge: Mechanical forces acting on T cells immobilized via the TCR complex can trigger TCR signaling. *Journal of Immunology*, 184(11), 5959. <https://doi.org/10.4049/jimmunol.0900775>
- Liao, Y., Smyth, G. K., & Shi, W. (2014). featureCounts: An efficient general purpose program for assigning sequence reads to genomic features. *Bioinformatics*, 30(7), 923–930. <https://doi.org/10.1093/bioinformatics/btt656>
- Liu, C. S. C., Raychaudhuri, D., Paul, B., Chakrabarty, Y., Ghosh, A. R., Rahaman, O., & Ganguly, D. (2018). Cutting edge: Piezo1 mechanosensors optimize human T cell activation. *Journal of Immunology*, 200(4), 1255–1260. <https://doi.org/10.4049/jimmunol.1701118>
- Livak, K. J., & Schmittgen, T. D. (2001). Analysis of relative gene expression data using real-time quantitative PCR and the 2^{- $\Delta\Delta$ CT} method. *Methods*, 25(4), 402–408. <https://doi.org/10.1006/meth.2001.1262>
- Lou, Z., Billadeau, D. D., Savoy, D. N., Schoon, R. A., & Leibson, P. J. (2001). A role for a RhoA/ROCK/LIM-kinase pathway in the regulation of cytotoxic lymphocytes. *Journal of Immunology*, 167(10), 5749–5757. <https://doi.org/10.4049/jimmunol.167.10.5749>
- Ma, Z., & Finkel, T. H. (2010). T cell receptor triggering by force. *Trends in Immunology*, 31(1), 1–6. <https://doi.org/10.1016/j.it.2009.09.008>
- Macián, F., García-Cózar, F., Im, S. H., Horton, H. F., Byrne, M. C., & Rao, A. (2002). Transcriptional mechanisms underlying lymphocyte tolerance. *Cell*, 109(6), 719–731. [https://doi.org/10.1016/s0092-8674\(02\)00767-5](https://doi.org/10.1016/s0092-8674(02)00767-5)
- McCaffrey, P. G., Luo, C., Kerppola, T. K., Jain, J., Badalian, T. M., Ho, A. M., Burgeon, E., Lane, W. S., Lambert, J. N., Curran, T., Verdine, G. L., Rao, A., & Hogan, P. G. (1993). Isolation of the cyclosporin-sensitive T cell transcription factor NFATp. *Science*, 262(5134), 750–754. <https://doi.org/10.1126/science.8235597>
- Nicoli, F., Papagno, L., Frere, J. J., Cabral-Piccin, M. P., Clave, E., Gostick, E., & Appay, V. (2018). Naïve CD8⁺ T-Cells engage a versatile metabolic program upon activation in humans and differ energetically from memory CD8⁺ T-cells. *Frontiers in Immunology*, 9(2736), 1–12. <https://doi.org/10.3389/fimmu.2018.02736>
- Northrop, J. P., Ho, S. N., Chen, L., Thomas, D. J., Timmerman, L. A., Nolan, G. P., & Crabtree, G. R. (1994). NF-AT components define a family of transcription factors targeted in T-cell activation. *Nature*, 369(6480), 497–502. <https://doi.org/10.1038/369497a0>
- Palazon, A., Goldrath, A. W., Nizet, V., & Johnson, R. S. (2014). HIF transcription factors, inflammation, and immunity. *Immunity*, 41(4), 518–528. <https://doi.org/10.1016/j.immuni.2014.09.008>
- Piroth, L., Cottenet, J., Mariet, A. S., Bonniaud, P., Blot, M., Tubert-Bitter, P., & Quantin, C. (2021). Comparison of the characteristics, morbidity, and mortality of COVID-19 and seasonal influenza: A nationwide, population-based retrospective cohort study. *The Lancet Respiratory Medicine*, 9(3), 251–259. [https://doi.org/10.1016/s2213-2600\(20\)30527-0](https://doi.org/10.1016/s2213-2600(20)30527-0)
- Ranade, S. S., Qiu, Z., Woo, S.-H., Hur, S. S., Murthy, S. E., Cahalan, S. M., & Patapoutian, A. (2014). Piezo1, a mechanically activated ion channel, is required for vascular development in mice. *Proceedings of the National Academy of Sciences of United States of America*, 111(28), 10347–10352. <https://doi.org/10.1073/pnas.1409233111>
- Robinson, M. D., McCarthy, D. J., & Smyth, G. K. (2010). edgeR: A bioconductor package for differential expression analysis of digital gene expression data. *Bioinformatics*, 26(1), 139–140. <https://doi.org/10.1093/bioinformatics/btp616>
- Sadoshima, J., & Izumo, S. (1997). The cellular and molecular response of cardiac myocytes to mechanical stress. *Annual Review of Physiology*, 59, 551–571. <https://doi.org/10.1146/annurev.physiol.59.1.551>
- Schoen, K., Horvat, N., Guerreiro, N. F. C., de Castro, I., & de Giassi, K. S. (2019). Spectrum of clinical and radiographic findings in patients with diagnosis of H1N1 and correlation with clinical severity. *BMC Infectious Diseases*, 19(1), 964. <https://doi.org/10.1186/s12879-019-4592-0>
- Solis, A. G., Bielecki, P., Steach, H. R., Sharma, L., Harman, C. C. D., Yun, S., & Flavell, R. A. (2019). Mechanosensation of cyclical force by

- PIEZO1 is essential for innate immunity. *Nature*, 573(7772), 69–74. <https://doi.org/10.1038/s41586-019-1485-8>
- Takemoto, K., Ishihara, S., Mizutani, T., Kawabata, K., & Haga, H. (2015). Compressive stress induces dephosphorylation of the myosin regulatory light chain via RhoA phosphorylation by the adenylyl cyclase/protein kinase A signaling pathway. *PLoS One*, 10(3), e0117937. <https://doi.org/10.1371/journal.pone.0117937>
- Teramura, T., Takehara, T., Onodera, Y., Nakagawa, K., Hamanishi, C., & Fukuda, K. (2012). Mechanical stimulation of cyclic tensile strain induces reduction of pluripotent related gene expressions via activation of Rho/ROCK and subsequent decreasing of AKT phosphorylation in human induced pluripotent stem cells. *Biochemical and Biophysical Research Communications*, 417(2), 836–841. <https://doi.org/10.1016/j.bbrc.2011.12.052>
- Tharoux, P. L., Bukoski, R. C., Rocha, P. N., Crowley, S. D., Ruiz, P., Nataraj, C., & Coffman, T. M. (2003). Rho kinase promotes alloimmune responses by regulating the proliferation and structure of T cells. *Journal of Immunology*, 171(1), 96–105. <https://doi.org/10.4049/jimmunol.171.1.96>
- Wahl, A., Dinet, C., Dillard, P., Nassereddine, A., Puech, P. H., Limozin, L., & Sengupta, K. (2019). Biphasic mechanosensitivity of T cell receptor-mediated spreading of lymphocytes. *Proceedings of the National Academy of Sciences of the United States of America*, 116(13), 5908–5913. <https://doi.org/10.1073/pnas.1811516116>
- Walczak-Drzewiecka, A., Ratajewski, M., Wagner, W., & Dastyk, J. (2008). HIF-1 α is up-regulated in activated mast cells by a process that involves calcineurin and NFAT. *Journal of Immunology*, 181(3), 1665–1672. <https://doi.org/10.4049/jimmunol.181.3.1665>
- Wang, R., Dillon, C. P., Shi, L. Z., Milasta, S., Carter, R., Finkelstein, D., & Green, D. R. (2011). The transcription factor Myc controls metabolic reprogramming upon T lymphocyte activation. *Immunity*, 35(6), 871–882. <https://doi.org/10.1016/j.immuni.2011.09.021>
- Wu, C., Orozco, C., Boyer, J., Leglise, M., Goodale, J., Batalov, S., & Su, A. I. (2009). BioGPS: An extensible and customizable portal for querying and organizing gene annotation resources. *Genome Biology*, 10(11), R130. <https://doi.org/10.1186/gb-2009-10-11-r130>
- Zheng, H. Y., Xu, M., Yang, C. X., Tian, R. R., Zhang, M., Li, J. J., & Zheng, Y. T. (2020). Longitudinal transcriptome analyses show robust T cell immunity during recovery from COVID-19. *Signal Transduction and Targeted Therapy*, 5(1), 294. <https://doi.org/10.1038/s41392-020-00457-4>

SUPPORTING INFORMATION

Additional supporting information may be found in the online version of the article at the publisher's website.

How to cite this article: Yassouf, M. Y., Zhang, X., Huang, Z., Zhai, D., Sekiya, R., Kawabata, T., & Li, T.-S. (2022). Biphasic effect of mechanical stress on lymphocyte activation. *Journal of Cellular Physiology*, 237, 1521–1531. <https://doi.org/10.1002/jcp.30623>

公益財団法人日中医学協会
TEL 03-5829-9123
FAX 03-3866-9080
〒101-0032 東京都千代田区岩本町 1-4-3
住 泉 K M ビ ル 6 階
URL : <https://www.jpcnma.or.jp/>